

Performance Evaluation of Arizona's LTPP SPS-9 Project: Strategic Study of Flexible Pavement Mix Design Factors



Arizona Department of Transportation Research Center

Performance Evaluation of Arizona's LTPP SPS-9 Project: Strategic Study of Flexible Pavement Mix Design Factors

SPR-396-9B
January 2016

Prepared by:

Jason Puccinelli
Nichols Consulting Engineers
1885 S. Arlington Avenue, Suite 11
Reno, NV 89505-3370

Steven M. Karamihas
The University of Michigan Transportation Research Institute
2901 Baxter Road
Ann Arbor, MI 48109

Sam Shih-Hsien Yang, Jonathan Minassian,
and Kevin Senn
Nichols Consulting Engineers
1885 S. Arlington Avenue, Suite 11
Reno, NV 89505-3370

Published by

Arizona Department of Transportation
206 S. 17th Avenue
Phoenix, AZ 85007
In cooperation with
U.S. Department of Transportation
Federal Highway Administration

This report was funded in part through grants from the Federal Highway Administration, U.S. Department of Transportation. The contents of this report reflect the views of the authors, who are responsible for the facts and the accuracy of the data, and for the use or adaptation of previously published material, presented herein. The contents do not necessarily reflect the official views or policies of the Arizona Department of Transportation or the Federal Highway Administration, U.S. Department of Transportation. This report does not constitute a standard, specification, or regulation. Trade or manufacturers' names that may appear herein are cited only because they are considered essential to the objectives of the report. The U.S. government and the State of Arizona do not endorse products or manufacturers.

Technical Report Documentation Page

1. Report No. FHWA-AZ-16-396(9B)		2. Government Accession No.		3. Recipient's Catalog No.	
4. Title and Subtitle Performance Evaluation of Arizona's LTPP SPS-9 Project: Strategic Study of Flexible Pavement Mix Design Factors				5. Report Date January 2016	
				6. Performing Organization Code	
7. Author(s) Jason Puccinelli, Steven M. Karamihas, Sam Shih-Hsien Yang, Jonathan Minassian, and Kevin Senn				8. Performing Organization Report No.	
9. Performing Organization Name and Address Nichols Consulting Engineers 1885 South Arlington Avenue Suite 111 Reno, NV 89509-3370 The University of Michigan Transportation Research Institute 2901 Baxter Road Ann Arbor, MI 48109				10. Work Unit No. (TRAIS)	
				11. Contract or Grant No. SPR 000-1(147) 396-9B	
12. Sponsoring Agency Name and Address Arizona Department of Transportation 206 S. 17th Avenue Phoenix, AZ 85007				13. Type of Report and Period Covered	
				14. Sponsoring Agency Code	
15. Supplementary Notes Prepared in cooperation with the US Department of Transportation, Federal Highway Administration					
16. Abstract As part of the Long Term Pavement Performance (LTPP) Program, the Arizona Department of Transportation (ADOT) constructed five Specific Pavement Studies 9 (SPS-9) test sections on U.S. Route 93 near Kingman. This project, SPS-9B, studied the effect of asphalt specifications and mix designs on flexible pavements, specifically comparing Superpave mix designs with commonly used agency designs. Opened to traffic in 1992, the project was monitored at regular intervals until the pavement was rehabilitated in 2006. Surface distress, profile, and deflection data collected throughout the life of the pavement were used to evaluate the performance of various flexible pavement design features, layer configurations, and thickness. In terms of structural cracking and smoothness, the agency standard mix design performed better than the Superpave mix designs in this study. This report documents the analyses conducted as well as practical findings and lessons learned that will be of interest to ADOT.					
17. Key Words LTPP, pavement performance, Superpave mix, profile, distress, FWD, flexible, AC, deflections, roughness, backcalculation		18. Distribution Statement Document is available to the U.S. public through the National Technical Information Service, Springfield, VA 22161		23. Registrant's Seal	
19. Security Classification Unclassified	20. Security Classification Unclassified	21. No. of Pages 75	22. Price		

SI* (MODERN METRIC) CONVERSION FACTORS

APPROXIMATE CONVERSIONS TO SI UNITS

Symbol	When You Know	Multiply By	To Find	Symbol
LENGTH				
in	inches	25.4	millimeters	mm
ft	feet	0.305	meters	m
yd	yards	0.914	meters	m
mi	miles	1.61	kilometers	km
AREA				
in ²	square inches	645.2	square millimeters	mm ²
ft ²	square feet	0.093	square meters	m ²
yd ²	square yard	0.836	square meters	m ²
ac	acres	0.405	hectares	ha
mi ²	square miles	2.59	square kilometers	km ²
VOLUME				
fl oz	fluid ounces	29.57	milliliters	mL
gal	gallons	3.785	liters	L
ft ³	cubic feet	0.028	cubic meters	m ³
yd ³	cubic yards	0.765	cubic meters	m ³
NOTE: volumes greater than 1000 L shall be shown in m ³				
MASS				
oz	ounces	28.35	grams	g
lb	pounds	0.454	kilograms	kg
T	short tons (2000 lb)	0.907	megagrams (or "metric ton")	Mg (or "t")
TEMPERATURE (exact degrees)				
°F	Fahrenheit	5 (F-32)/9 or (F-32)/1.8	Celsius	°C
ILLUMINATION				
fc	foot-candles	10.76	lux	lx
fl	foot-Lamberts	3.426	candela/m ²	cd/m ²
FORCE and PRESSURE or STRESS				
lbf	poundforce	4.45	newtons	N
lbf/in ²	poundforce per square inch	6.89	kilopascals	kPa

APPROXIMATE CONVERSIONS FROM SI UNITS

Symbol	When You Know	Multiply By	To Find	Symbol
LENGTH				
mm	millimeters	0.039	inches	in
m	meters	3.28	feet	ft
m	meters	1.09	yards	yd
km	kilometers	0.621	miles	mi
AREA				
mm ²	square millimeters	0.0016	square inches	in ²
m ²	square meters	10.764	square feet	ft ²
m ²	square meters	1.195	square yards	yd ²
ha	hectares	2.47	acres	ac
km ²	square kilometers	0.386	square miles	mi ²
VOLUME				
mL	milliliters	0.034	fluid ounces	fl oz
L	liters	0.264	gallons	gal
m ³	cubic meters	35.314	cubic feet	ft ³
m ³	cubic meters	1.307	cubic yards	yd ³
MASS				
g	grams	0.035	ounces	oz
kg	kilograms	2.202	pounds	lb
Mg (or "t")	megagrams (or "metric ton")	1.103	short tons (2000 lb)	T
TEMPERATURE (exact degrees)				
°C	Celsius	1.8C+32	Fahrenheit	°F
ILLUMINATION				
lx	lux	0.0929	foot-candles	fc
cd/m ²	candela/m ²	0.2919	foot-Lamberts	fl
FORCE and PRESSURE or STRESS				
N	newtons	0.225	poundforce	lbf
kPa	kilopascals	0.145	poundforce per square inch	lbf/in ²

*SI is the symbol for the International System of Units. Appropriate rounding should be made to comply with Section 4 of ASTM E380. (Revised March 2003)

Contents

EXECUTIVE SUMMARY	1
CHAPTER 1. INTRODUCTION	3
CHAPTER 2. SPS-9B DEFLECTION ANALYSIS.....	15
Analysis of Deflection Data.....	15
Maximum Deflection, Minimum Deflection, and AREA Value	15
Backcalculation Using the AASHTO Design Guide Procedure	19
Backcalculation Using Evercalc Software	22
CHAPTER 3. SPS-9B DISTRESS ANALYSIS	27
AC Distress Types.....	27
Research Approach.....	28
Overall Performance Trend Observations.....	30
Key Findings from the SPS-9B Distress Analysis	37
CHAPTER 4. SPS-9B ROUGHNESS ANALYSIS	39
Profile Data Synchronization	39
Data Extraction	39
Cross Correlation	40
Synchronization	41
Data Quality Screening	41
Summary Roughness Values.....	44
Profile Analysis Tools	47
Detailed Observations	50
Summary.....	60
CHAPTER 5. CONCLUSIONS AND RECOMMENDATIONS	63
REFERENCES.....	65
APPENDIX: ROUGHNESS VALUES.....	67

LIST OF FIGURES

Figure 1. Structural Layers of SPS-9B (040900 and 04A900)	3
Figure 2. Location of SPS-9B Test Sections 040900 and 04A900	5
Figure 3. SPS-9B Test Section Layout	6
Figure 4. SPS-9B Test Section Layout and Details	7
Figure 5. Average Normalized D_{max} by Test Section	16
Figure 6. Average Normalized D_{min} by Test Section	17
Figure 7. AREA Values by Test Section	18
Figure 8. Backcalculated AC Modulus by Test Section (Evercalc Method)	24
Figure 9. Backcalculated Subgrade Resilient Modulus by Test Section (Evercalc Method)	24
Figure 10. Structural Damage Trends for SPS-9B Test Sections	31
Figure 11. Environmental Damage Trends for SPS-9B Test Sections	33
Figure 12. Structural Damage Index Summary	34
Figure 13. Environmental Damage Index Summary	35
Figure 14. Rutting Index Summary	36
Figure 15. IRI Progression, Section 04A901	45
Figure 16. IRI Progression, Section 040902	45
Figure 17. IRI Progression, Section 04A902	46
Figure 18. IRI Progression, Section 040903	46
Figure 19. IRI Progression, Section 04A903	47
Figure 20. Periodic Chatter in Elevation Profiles from Section 04A901, Left Side	51
Figure 21. Pavement Scuff in the Left Wheelpath, Section 04A901	52
Figure 22. Narrow Downward Spikes in Elevation Profile, Section 040903, Visit 13	57
Figure 23. Summary of IRI Ranges	61
Figure 24. Comparison of HRI to MRI	68

LIST OF TABLES

Table 1. Test Section Layer Thickness.....	4
Table 2. Inputs for LTPP Bind v. 3.1	8
Table 3. SPS-9B Mix Design Properties	9
Table 4. Aggregate Properties for Agency Standard Marshall Mix (04A901)	10
Table 5. SPS-9B Mix and Binder Properties (As Constructed).....	11
Table 6. Climatic Information for SPS-9B	12
Table 7. Dynamic Modulus (E*)	13
Table 8. SPS-9B Traffic-Loading Summary	14
Table 9. General Trends in D ₀ and AREA Values (Mahoney 1995).....	18
Table 10. Structural Parameter Statistics for SPS-9B	21
Table 11. Backcalculation Seed Value and Modulus Range.....	22
Table 12. Backcalculation Moduli Statistics for SPS-9B Test Sections	23
Table 13. Flexible Pavement Distress Types and Failure Mechanisms	28
Table 14. Profile Measurement Visits to the SPS-9B Site	39
Table 15. Selected Repeats, Section 04A901.....	42
Table 16. Selected Repeats, Section 040902	42
Table 17. Selected Repeats, Section 04A902.....	43
Table 18. Selected Repeats, Section 040903	43
Table 19. Selected Repeats, Section 04A903.....	43
Table 20. Roughness Values.....	68

List of Acronyms and Abbreviations

AASHTO	American Association of State Highway and Transportation Officials
AB	aggregate base
AC	asphalt concrete
ADOT	Arizona Department of Transportation
COV	coefficient of variation
D_{max}	maximum deflection
D_{min}	minimum deflection
E^*	dynamic modulus
E_p	effective pavement modulus
ESAL	equivalent single axle load
FWD	falling weight deflectometer
HRI	Half-car Roughness Index
IRI	International Roughness Index
ksi	kips per square inch
lbf	pound force
LTPP	Long Term Pavement Performance
M_R	resilient modulus
MP	milepost
MRI	Mean Roughness Index
PG	performance grade
PSD	power spectral density
psi	pounds per square inch
RN	Ride Number
SHRP	Strategic Highway Research Program
SN	structural number
SN_{eff}	effective structural number
SPS	Specific Pavement Studies

EXECUTIVE SUMMARY

As part of the Long Term Pavement Performance (LTPP) Program, the Arizona Department of Transportation (ADOT) constructed five Specific Pavement Studies 9 (SPS-9) test sections on U.S. Route 93 near Kingman. This project, SPS-9B, studied the effect of asphalt specifications and mix designs on flexible pavements, specifically comparing Superpave mix designs with commonly used agency designs. The SPS-9B test sections (040900 and 04A900) consisted of three pavement mixes with two replicate sections. Sections 04A902 and 04A903 were both Level 1 Superpave mix designs with 25-mm (1-inch) aggregate. Sections 040902 and 040903 were also Level 1 Superpave mix designs but were composed of 19-mm (3/4-inch) aggregate. Both Superpave mixes were performance grade (PG) 64-16. Test section 04A901 was an agency standard mix using the Marshall mix design and containing 19-mm aggregate. Construction of all five sections occurred between November 1992 and August 1993, and all five sections were placed out of study in June 2006.

This report provides general information about the project location, including climate, traffic, and subgrade conditions, as well as details about the mix designs of each test section. The five SPS-9B test sections were constructed consecutively and exposed to the same traffic loading, climate, and subgrade conditions, which allowed for direct comparisons between layer configurations and design features without the confounding effects introduced by different in situ conditions.

Two of the sections received a slurry seal coat in 2002, which altered the profile features significantly. The seal coat temporarily smoothed surface deterioration but did not otherwise significantly improve environmental cracking. The sections not receiving the slurry seal had a very poor surface condition at the end of their service lives. Most sections had a clear increase in the magnitude of environmental distress approximately 10 years after construction. The slurry seal was applied after considerable cracking was present. It would likely have been more effective at slowing deterioration if it had been placed a few years earlier, prior to the development of cracking (possibly at the first sign of raveling).

The vast majority of sections showed significant growth in longitudinal cracking, and consequently fatigue cracking. This occurred nine to 10 years after construction, with the rate of crack growth then slowing until the sections were placed out of study. After 11 years, there was no significant difference in structural cracking between the 19-mm and 25-mm mixes. All sections performed well with regard to rut resistance. Rutting would not have triggered a rehabilitation event for any section.

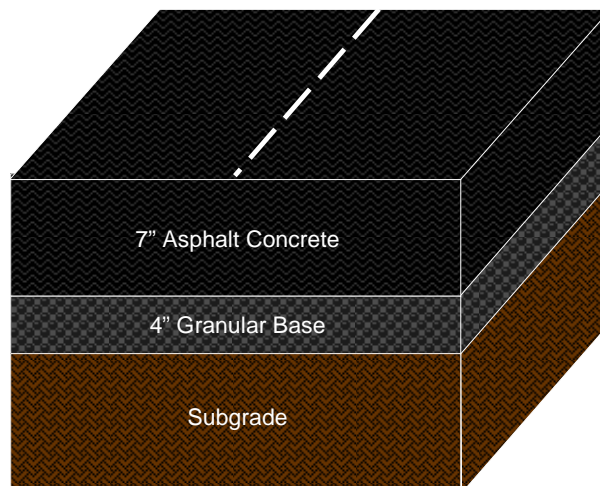
The study compared the performance of the Superpave mix designs for asphalt pavements to the agency standard mix design and found that the agency standard mix design had better performance in terms of both structural cracking and smoothness. These findings can provide a foundation for future design decisions, but it should be recognized that Superpave mix designs and construction practices have evolved over the past two decades. In addition, site-specific conditions and construction issues may have negatively affected the performance of the Superpave mixes in this study.

CHAPTER 1. INTRODUCTION

Understanding how design features contribute to long-term pavement performance can be extremely valuable to pavement designers looking to optimize resources and improve overall performance. This study's objectives were to document the overall performance trends of the Specific Pavement Studies 9 (SPS-9) project, identify key differences in performance between the various asphalt specifications and mix designs, and document key findings that would be useful to the Arizona Department of Transportation (ADOT).

This report provides the results of surface distress, deflection, and profile analyses for the Long Term Pavement Performance (LTPP) SPS-9 site near Kingman (the SPS-9B project). The SPS-9B sites were designed to study the effect of asphalt specifications and mix designs on flexible pavements, specifically comparing Superpave mix designs with commonly used agency designs. The two SPS-9B projects discussed in this report (040900 and 04A900) consist of five newly constructed sections. These sections were constructed in conjunction with the SPS-1 project at the same location. The five SPS-9B test sections consisted of three pavement mixes with two replicate sections. Sections 04A902 and 04A903 were both Level 1 Superpave mix designs with 25-mm (1-inch) aggregate. Sections 040902 and 040903 were also Level 1 Superpave mix designs but were composed of 19-mm (3/4-inch) aggregate. Both Superpave mixes were performance grade (PG) 64-16. Test section 04A901 was an agency standard mix using the Marshall mix design and containing 19-mm aggregate.

All five SPS-9B test sections had the same thickness design; each consisted of approximately 7 inches of asphalt concrete laid over 4 inches of granular base placed on top of subgrade. Figure 1 depicts a structural cross section of the sites as originally constructed.



Note: Layer thicknesses are approximate. Sites 040902 and 04A902 received a 0.5-inch slurry seal in 2002 (not shown).

Figure 1. Structural Layers of SPS-9B (040900 and 04A900)

After original construction in 1992 to 1993, the following maintenance activities were performed:

- **040902 (Superpave mix, Level 1, PG 64-16, 19 mm):** Slurry seal in 2002.
- **040903 (Superpave mix, Level 1, PG 64-16, 19 mm):** No rehabilitation or maintenance conducted.
- **04A901 (agency standard mix, 19 mm):** No rehabilitation or maintenance conducted.
- **04A902 (Superpave mix, Level 1, PG 64-16, 25 mm):** Crack seal in 2001; slurry seal in 2002.
- **04A903 (Superpave mix, Level 1, PG 64-16, 25 mm):** No rehabilitation or maintenance conducted.

All test sections were placed out of study due to reconstruction in the summer of 2006.

Table 1 lists the test section structural properties in further detail. As previously mentioned, Sections 040902 and 04A902 received a 0.5-inch slurry seal in 2002. The LTPP construction report (Nichols Consulting Engineers 1997) provides more detail on the layout and structural properties of the site.

Table 1. Test Section Layer Thickness

Section	Granular Base Thickness (inches)	Asphalt Concrete Thickness (inches)
040902	4	7*
040903	4	6.6
04A901	4	6.9
04A902	4	6.5*
04A903	4	6.7

*0.5-inch slurry seal applied in 2002.

The test pavements were constructed on northbound U.S. Route 93 in Mohave County, Arizona, from November 1992 to August 1993. The site extends from milepost 53.23 to milepost 46.43, which is north of Kingman and south of the Nevada/Arizona border. The terrain surrounding the test section is slightly rolling, and the roadway is straight with grades reaching 3 percent in some areas. The soil is covered with various desert-type brush and small trees. Low foothills surround the test section in the distance. The approximate elevation of the test section is 3523 ft, with a latitude of 35° 23' and longitude of -114° 15'. The location and layout of the SPS-9B project are shown in Figures 2 through 4. The five SPS-9B test sections were constructed concurrently with the SPS-1 project. The performance of the SPS-1 project is discussed in a separate report (Puccinelli et al. 2012).

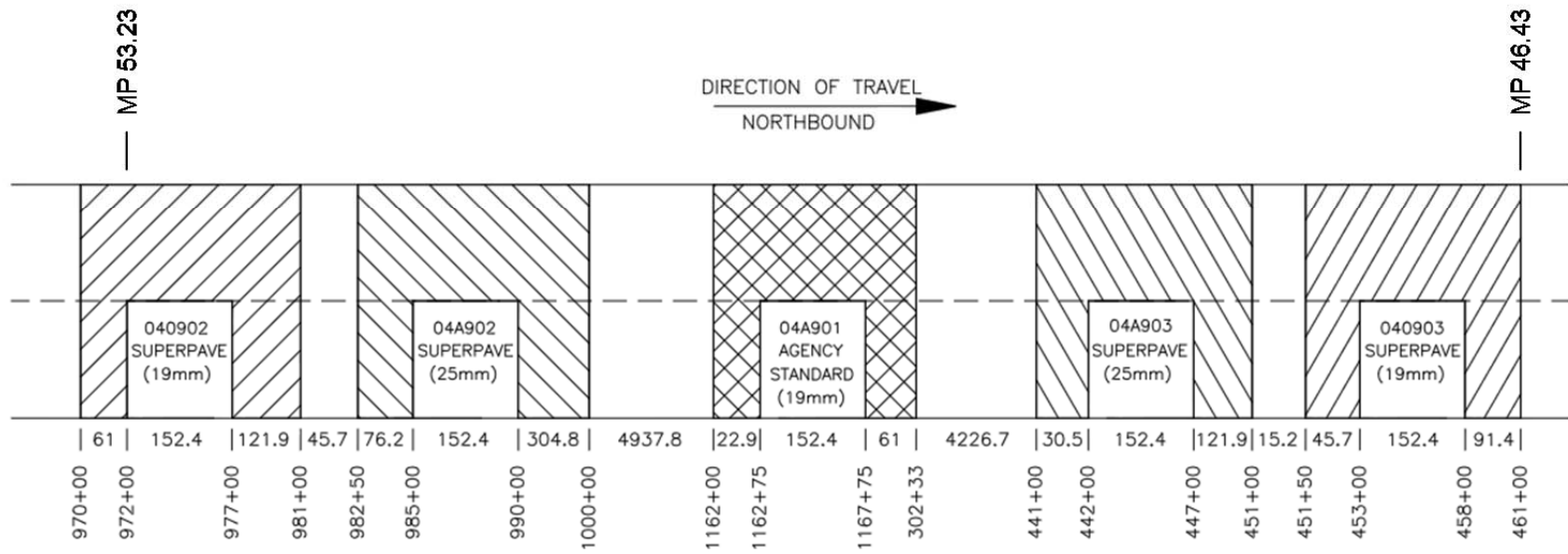
The test sections are located entirely on a shallow fill of native material. The subgrade and embankment material are a coarse-grained silty sand with gravel and cobbles.

During paving, both Superpave mixtures were susceptible to segregation. This segregation was attributed to the coarseness of the mixes and to worn kickback paddles on the paver. This caused areas with significant surface voids. However, ADOT reported that after three months of traffic, the surfaces of the Superpave mixtures appeared less bony and were no longer rich-looking. At this point, segregation did not seem to be a problem.



**Figure 2. Location of SPS-9B Test Sections 040900 and 04A900
(Courtesy of Google Maps)**

SPS-9 TEST SECTION LAYOUT
 040900 & 04A900
 KINGMAN, ARIZONA
 US-93 NORTHBOUND
 09/28/00



NOTES: STATIONS IN FEET (Per Plans)
 DISTANCES IN METERS

EQUATION 1167+93.75 Bk = 300+51.82 Ahd

Figure 3. SPS-9 Test Section Layout

Within the SPS-9 experiment, early projects such as 040900 and 04A900 were designated SPS-9P, with the “P” standing for pilot. The test sections were designed and constructed according to interim Superpave specifications then available, some of which were revised following construction of the SPS-9P projects. Additional changes internal to the LTPP program regarding materials sampling and testing requirements for SPS-9 applied to projects constructed later and not to the SPS-9P projects. These changes were not unexpected, and the SPS-9P sections were nominated and selected with the understanding that Superpave modifications would occur. It was determined by the Strategic Highway Research Program (SHRP) and by the participating state and provincial highway agencies that it was more important to develop experience implementing Superpave specifications than to wait until everything had been finalized.

Station	Distance	SHRP ID	Original Pavement Configuration						
			AC			Base and Subbase		Base and Subbase	
(ft)	(m)		Thick (in)	Type	Mix Design	Binder Grade	Thick (in)	Type	Type
972+00	152.4	040902	7.0	Dense Grade AC	Superpave Level I: ¾ in (19mm)	AC-30 (=PG 64-16)	4.0	Crush Stone, Gravel/Slag	Silty Sand
977+00 985+00			04A902	6.5	Dense Grade AC	Superpave Level I: 1 in (25mm)	AC-30 (=PG 64-16)	4.0	Crushed Gravel
990+00									
1162+75	152.4	04A901	6.9	Dense Grade AC	ADOT Standard (Marshall Design): ¾ in (19mm)	AC-30 (=PG 64-16)	4.0	Crushed Gravel	Coarse Grained Soil: Silty Sand with Gravel
1167+75									
1309+42	152.4	04A903	6.7	Dense Grade AC	Superpave Level I: 1 in (25mm)	AC-30 (=PG 64-16)	4.0	Crushed Gravel	Coarse Grained Soil: Well Graded Gravel with Silt and Sand
1314+42 1320+42			040903	7.0	Dense Grade AC	Superpave Level I: ¾ in (19mm)	AC-30 (=PG 64-16)	4.0	Crush Stone, Gravel/Slag
1325+42									

Figure 4. SPS-9P Test Section Layout and Details

As mentioned previously, the five test sections were used to compare three different scenarios, with two replicate tests. The test sections were constructed using different asphalt specifications and mix designs. Sections 040902 and 040903 were Superpave Level 1 mixes with 19-mm gradations, Sections 04A902 and 04A903 were Superpave Level 1 mixes with 25-mm gradations, and Section 04A901 was a standard agency mix using a 75-blow Marshall mix design with a 19-mm gradation. However, because the asphalt binder, AC-30, met both the agency standard and the Superpave design specification, it was used for all five test sections. Using the LTPP Bind 3.1 software, the recommended binder for this project site was PG 76-10. The inputs used in the program are shown in Table 2.

Table 2. Inputs for LTPP Bind v. 3.1

Latitude	35.2°
Lowest yearly air temperature	-8.8° C
Yearly degree-days greater than 10° C	3884
Low air temperature standard deviation	3.1° C
Desired reliability	98%
Depth of layer	0 mm
Traffic speed	Fast
Traffic loading	Up to 3 million ESALs

Table 3 shows the mix design properties of each test section, Table 4 shows the mix property test results, and Table 5 shows the mix and binder properties as constructed. The Superpave mix design required an AC content of approximately 5 percent to achieve 4.0 percent air voids. This was noticeably more binder than the agency mix design required to achieve the same amount of air voids. In fact, the agency mix with a 5 percent AC content would have yielded only 2 to 3 percent air voids (Sebaaly et al. 2001).

Table 3. SPS-9B Mix Design Properties

Property	040902	040903	04A901		04A902	04A903
			Marshall	Specification		
Mix type	Superpave	Superpave	Marshall	Specification	Superpave	Superpave
Asphalt binder	AC-30 PG 64-16	AC-30 PG 64-16	AC-30	N/A	AC-30 PG 64-16	AC-30 PG 64-16
Maximum specific gravity	2.509	2.509	N/A	N/A	2.523	2.523
Bulk specific gravity	2.406	2.406	N/A	N/A	2.422	2.422
Specific gravity of aggregate blend	2.670	2.670	N/A	N/A	2.683	2.683
Aggregate effective specific gravity	2.724	2.724	N/A	N/A	2.727	2.727
Specific gravity of binder (G_b)	1.03	1.03	N/A	N/A	1.03	1.03
Asphalt content (%)	5.2	5.2	4.1	N/A	4.9	4.9
Air voids (%)	4.1	4.1	5.6	5.3–5.7	4.0	4.0
Mineral aggregate air voids (%)	14.6	14.6	14.5	14.5–17.0	14.2	14.2
Voids filled with asphalt (%)	73.0	73.0	61.4	N/A	72.0	72.0
Asphalt absorption (%)	0.8	0.8	N/A	N/A	0.6	0.6
Effective asphalt content (%)	4.4	4.4	3.9	N/A	4.3	4.3
Marshall stability (lb)	3500	3500	5013	2990 min.	3800	3800
Immersion compression retention	N/A	N/A	83.9	50 min.	N/A	N/A
Number of blows	75	75	75	N/A	75	75
Marshall flow value (1 x 10 ⁻² inches)	15	15	10	N/A	17	17
Number of gyrations in Superpave Gyratory Compactor	113	113	113	N/A	113	113
Density (kg/m ³)	2406	2406	2385	N/A	2423	2423
Percentage of maximum specific gravity at initial number of gyrations (% G_{mm} @ N_{ini})	86.7	86.7	N/A	N/A	86.0	86.0
Percentage of maximum specific gravity at maximum number of gyrations (% G_{mm} @ N_{max})	98.3	98.3	N/A	N/A	98.2	98.2
Tensile strength ratio (%)	N/A	N/A	N/A	N/A	82.6	82.6

N/A: Not available.

Table 4. Aggregate Properties for Agency Standard Marshall Mix (04A901)

Property	Test Result	Specification
Bulk oven-dried specific gravity (combined)	2.673	2.35–2.85
Saturated surface-dry specific gravity (combined)	2.693	N/A
Apparent specific gravity (combined)	2.72	N/A
Asphalt absorption (combined) (%)	0.756	0–2.50
Sand equivalent	64	45 min.
Plasticity index	Nonplastic	N/A
Crushed faces	98	70 min.
LA abrasion test, 100 revolutions (% loss)	6	9 max.
LA abrasion test, 500 revolutions (% loss)	25	40 max.

N/A: Not available.

Table 5. SPS-9B Mix and Binder Properties (As Constructed)

	040902	040903	04A901	04A902	04A903
Mix type	Superpave	Superpave	Marshall	Superpave	Superpave
In situ density (kg/m³)	2335	2345	2191	2302	2311
Average core thickness (inches)	7.10	6.64	6.87	6.51	6.73
Maximum specific gravity	2.555	2.507	N/A	2.520	2.524
Average bulk specific gravity of cores	2.355	2.324	2.328	2.369	2.365
AASHTO T-283 tensile strength ratio	0.616	0.750	N/A	0.611	0.670
Asphalt content (%)	4.3	4.2	N/A	4.7	4.9
Abson ash content (%)	0.4	0.2	N/A	0.3	0.2
Air voids (%)	7.8	7.3	N/A	6.0	6.3
Coarse aggregate					
Bulk specific gravity	2.66	2.67	N/A	2.73	2.69
Asphalt absorption (%)	0.7	0.9		0.6	0.7
Fine aggregate					
Bulk specific gravity	2.64	2.62	N/A	2.62	2.63
Asphalt absorption (%)	1.0	1.1		1.3	1.3
Recovered asphalt cement					
Penetration at 25° C (mm)	31	33		54	35
Penetration at 46° C (mm)	144	161		258	150
Penetration index	1.6	1.4		1.5	2.0
Kinematic viscosity at 135° C (centistokes)	686	N/A	N/A	482	668
Absolute viscosity at 60° C (poise)	10,824	N/A		4144	8947
Specific gravity of AC	1.040	1.042	N/A	1.043	1.039
Gradation (percentage of aggregate passing metric sieves)					
37.5 mm	100	100		100	100
25.0 mm	100	100		96	95
19.0 mm	97	96		84	88
12.5 mm	67	69		70	74
9.5 mm	51	54	N/A	62	65
4.75 mm	33	35		43	46
2.00 mm	17	19		24	24
0.425 mm	8	10		12	11
0.180 mm	5	6		7	6
0.075 mm	2.6	3.6		4.0	4.0
Average M_R value					
at 5° C	9.827	11.5	11.99	9.175	10.655
at 25° C	3.18	3.125	4.2	2.91	3.425
at 40° C	0.94	0.955	1.55	0.935	1.165

N/A: Not available.

By LTPP definitions, the SPS-9 project site is a dry, no-freeze environment (Table 6). The temperature and precipitation information in Table 6 represents 40 years of recorded data collected at nearby weather stations. The solar radiation and humidity data were summarized from 14 years of on-site weather station data.

Table 6. Climatic Information for SPS-9B

	40-Year Average	40-Year Maximum	40-Year Minimum
Annual average daily mean temperature (°F)	67	71	62
Annual average daily maximum temperature (°F)	80	85	75
Annual average daily minimum temperature (°F)	53	58	49
Absolute maximum annual temperature (°F)	111	118	103
Absolute minimum annual temperature (°F)	22	30	8
Number of days per year above 32° F	130	168	89
Number of days per year below 32° F	22	53	4
Annual average freezing index (°F-days)	3	27	0
Annual average precipitation (inches)	8.1	17.5	3.1
Annual average daily mean solar radiation (W/ft ²)	21.3	39.8	1.1
Annual average daily maximum relative humidity (%)	54	66	45
Annual average daily minimum relative humidity (%)	18	23	14

The dynamic modulus (E^*) was calculated for the 040900/04A900 projects. The E^* values provided in Table 7 are estimates based on models originally developed by LaCroix et al. (2008) and implemented in the Resilient Modulus Artificial Neural Network model developed by Kim et al. (2011).

Table 7. Dynamic Modulus (E^*)

Layer	Temperature (°C)	Sample Age (Days)	Frequency					
			0.1	0.5	1	5	10	25
040902 & 040903 Superpave Level 1 (19-mm mix)	14	2	2133024	2477977	2610055	2875375	2972105	3084771
	40	2	810585	1162417	1328574	1727111	1897106	2114090
	70	2	148826	251661	314159	511830	621521	789076
	100	2	37396	56834	69375	114045	142670	192501
	130	2	18182	23472	26740	38054	45263	58006
04A902 & 04A903 Superpave Level 1 (25-mm mix)	14	1	2745733	3091657	3221097	3477140	3569411	3676340
	40	1	1241738	1680914	1876068	2320166	2501207	2726370
	70	1	252467	428412	530061	830738	986738	1213502
	100	1	51062	86030	108938	190313	241563	328605
	130	1	18811	27237	32660	52225	65080	88165
Standard Mix AC-30 (19-mm mix)	14	42	2987800	3328270	3454697	3703494	3792803	3896116
	40	42	1441150	1907156	2109790	2562672	2744469	2968617
	70	42	312803	525201	644927	989076	1162821	1410643
	100	42	60292	104683	133734	235942	299394	405597
	130	42	20048	30376	37122	61764	78071	107393

Table 8 summarizes the total equivalent single axle loads (ESALs) computed from traffic-loading information collected at the SPS-9 site. For 1993 and 2002, no monitoring traffic data were available. The ESAL value for 1993 was derived from estimates provided by ADOT. The significant reduction in ESALs after 2001 is due to the restriction of truck traffic on Hoover Dam implemented following September 11.

Table 8. SPS-9B Traffic-Loading Summary

Year	ESALs
1993	230,000*
1994	231,090
1995	252,299
1996	273,576
1997	260,773
1998	282,142
1999	299,002
2000	351,006
2001	380,213
2002	N/A
2003	52,847
2004	57,257
2005	46,917

*ADOT traffic estimate. No monitoring data available.

N/A: Not available.

Three analyses were conducted on the SPS-9B project to evaluate pavement performance: deflection, distress, and profile. The remaining chapters of this report address each analysis, including a description of the research approach along with performance comparisons between test sections, overall trends, a summary of the results, and key findings.

CHAPTER 2. SPS-9B DEFLECTION ANALYSIS

Falling weight deflectometer (FWD) data provide information about the overall strength (i.e., stiffness) of the pavement structure and individual layers. At the SPS-9B site, researchers used this information to evaluate changes with time or, as in the case of the asphalt-bound layers, temperature. The researchers conducted additional analyses to gain insight on how various design features affect structural performance.

ANALYSIS OF DEFLECTION DATA

Using the nondestructive FWD deflection testing data, researchers can identify the structural condition of the sections over their service life. In this chapter, three levels of analysis are presented. First, researchers produced the deflection profile plots of maximum deflection (D_0), minimum deflection (D_7/ D_8), and AREA value for all sections as a preliminary analysis to identify changes in the pavement and subgrade over time. Next, they backcalculated the subgrade resilient modulus (M_R), effective pavement modulus (E_p), and effective structural number (SN_{eff}) as outlined in the *AASHTO Guide for Design of Pavement Structures* (AASHTO 1993). Finally, they backcalculated asphalt concrete (AC) modulus and M_R using industry standard software.

MAXIMUM DEFLECTION, MINIMUM DEFLECTION, AND AREA VALUE

Maximum Deflections

The normalized average maximum deflection (D_0 , measured at the center of the FWD load plate, normalized to a load level of 9000 pounds and an AC mix temperature of 68° F) typically indicates the total stiffness of the pavement structure (surface and base) and the underlying subgrade. Increases in the normalized average maximum deflection (or D_{max}) observed over time may be due to weakening of the pavement structure, weakening of the subgrade, or both.

Figure 5 shows D_{max} results for each test section from the first round of testing to the last. Except for Section 04A901, the first round of testing for all sections was performed in February 1994. The first round of tests for section 04A901 was performed in January 1998. The last round of testing for all sections was performed in April 2005.

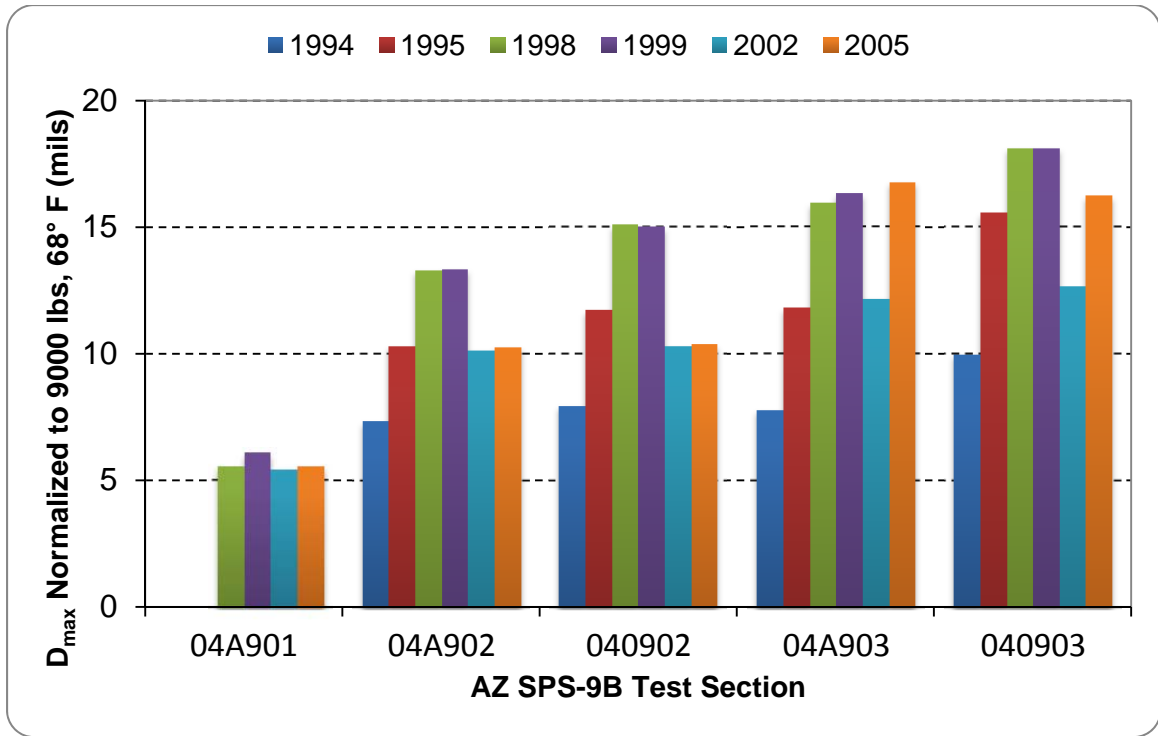


Figure 5. Average Normalized D_{max} by Test Section

Minimum Deflections

The minimum deflection (D_{min}) is observed in the sensor farthest from the loading plate, which for LTPP can be either sensor No. 7 or sensor No. 8, depending on the configuration used. D_{min} readings are also normalized to a standard 9000 pounds, but no temperature correction factor is applied. D_{min} readings are indicative of the subgrade characteristics. Figure 6 shows the D_{min} measurement from the first round of testing to the last. Four rounds of testing were conducted on Section 04A901, and six rounds of testing were conducted on the remaining sections. Similar deflection responses were observed in Sections 04A901, 04A903, and 040903, where the deflection value was higher than that measured in Sections 04A902 and 040902. The average D_{min} in Sections 04A901, 04A903, and 040903 was about 0.9 mils, and the average D_{min} in Sections 04A902 and 040902 was about 0.6 mils.

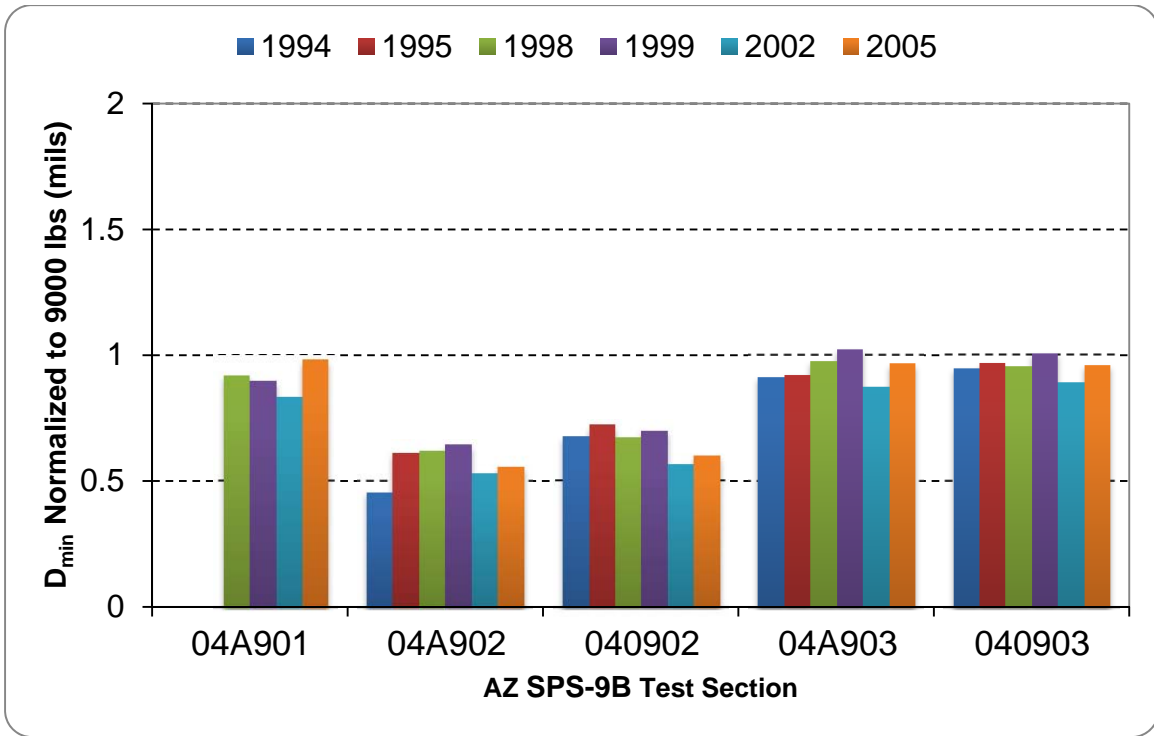


Figure 6. Average Normalized D_{min} by Test Section

AREA Value

The AREA parameter is commonly used as a means of quantifying the relative stiffness of a pavement section. The equation for the AREA value is (AASHTO 1993):

$$A = 6(D_0 + 2D_1 + 2D_2 + D_3)/D_0 \quad (\text{Eq. 1})$$

Where A = area value

D_0 = surface deflection at the center of the test load

D_1 = surface deflection at 12 inches

D_2 = surface deflection at 24 inches

D_3 = surface deflection at 36 inches

The AREA value is the normalized area of a slice taken through any deflection basin between the center of the loaded area and 36 inches. This area is said to be normalized because it is divided by the

maximum deflection, D_0 . The maximum value of the AREA parameter is 36 inches, which occurs when all four deflection values are equal. This would result from testing an extremely rigid section of pavement. The minimum AREA value is 11.02 inches, which would result from deflection measurements on a one-layer system of homogeneous material. This would imply that the pavement structure is of the same stiffness as the underlying soil. The state of Washington suggested that general trends in pavement condition can be concluded from the combination of AREA value and maximum deflection (Table 9) (Mahoney 1995).

Table 9. General Trends in D_0 and AREA Values (Mahoney 1995)

FWD-Based Parameter		Generalized Conclusions
AREA	D_{max}	
Low	Low	Weak structure, strong subgrade
Low	High	Weak structure, weak subgrade
High	Low	Strong structure, strong subgrade
High	High	Strong structure, weak subgrade

Figure 7 shows the average AREA values for the SPS-9B test sections over the years. As expected, the overall trend in AREA value was a decrease over time. This is because the structure strength decreased as distresses developed in the pavement.

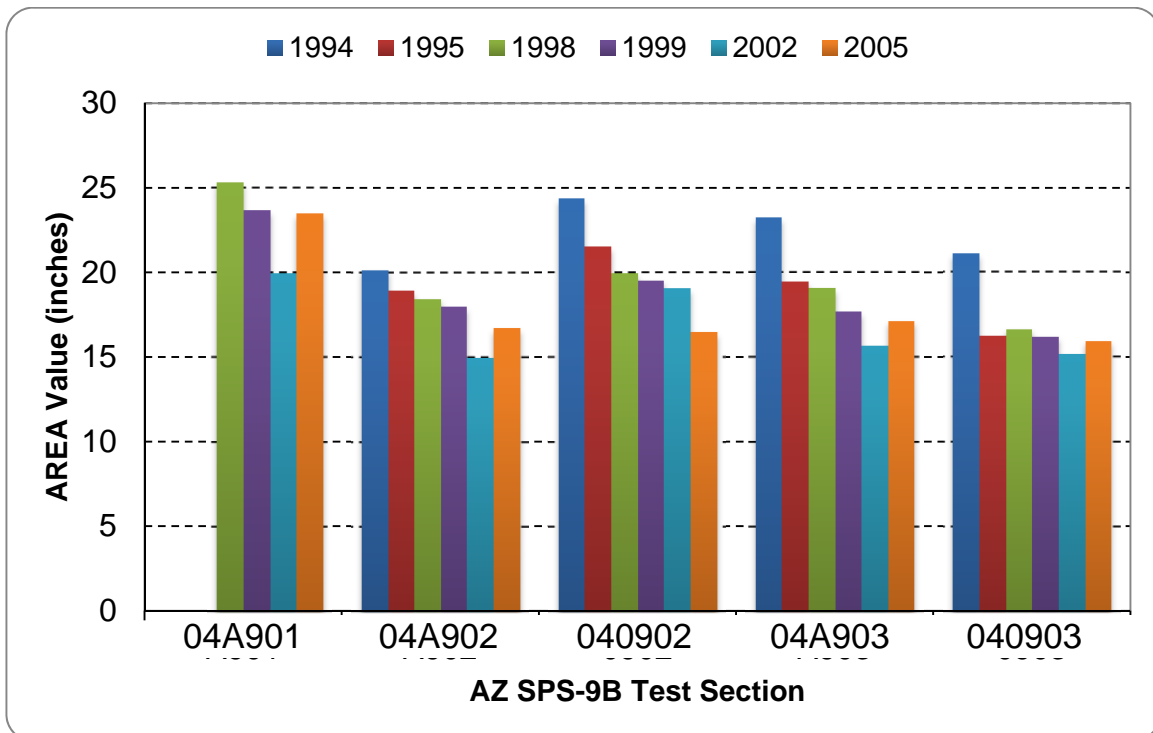


Figure 7. AREA Values by Test Section

Sections 04A902 and 04A903 were both constructed using Superpave Level I mix with 25-mm nominal aggregate size, but the AREA values are larger in Section 04A903 than in Section 04A902. In addition, the minimum deflection in 04A902 is smaller than in 04A903. This implies that the subgrade is stronger in 04A902 than in 04A903. Thus, the structure strength above the subgrade in 04A902 is much weaker than in 04A903. By contrast, Section 040903 has generally lower AREA values than Section 040902, indicating that 040903 is a stronger pavement overall.

BACKCALCULATION USING THE AASHTO DESIGN GUIDE PROCEDURE

The 1993 *AASHTO Guide for Design of Pavement Structures* (AASHTO 1993) outlines a procedure for calculating M_R , the effective modulus of all pavement layers above the subgrade, and SN_{eff} using measured deflection data. The deflections, which are measured at a distance of at least 0.7 times the radius of the stress bulb at the subgrade-pavement interface, are considered to reflect the deformation of the subgrade layer only and hence can be used to compute M_R . The backcalculated M_R can be calculated as:

$$M_R = \frac{(1 - \mu^2) P}{\pi r D_R} \quad (\text{Eq. 2})$$

Where M_R = backcalculated subgrade resilient modulus

μ = Poisson's ratio ($\mu = 0.5$ was assumed in the analysis)

P = applied load (lbf)

r = distance from the center of the load plate to D_r (inches)

D_r = pavement surface deflection at distance r from the center of the load plate (inches)

The radius of the stress bulb can be determined from the following equation:

$$a_e = \sqrt{a^2 + \left(D^3 \sqrt{\frac{E_P}{M_R}} \right)} \quad (\text{Eq. 3})$$

Where a_e = radius of the stress bulb at the subgrade-pavement interface (inches)

a = FWD load plate radius (inches)

D = total thickness of pavement layers (inches)

E_p = effective pavement modulus

M_R = backcalculated subgrade resilient modulus

To obtain E_p in this equation, the researchers used an equation linking the FWD deflection at the center plate (D_{max}), E_p , and M_R :

$$d_0 = 1.5Pa \left[\frac{1}{M_R \sqrt{1 + \left(\frac{D}{a} \sqrt{\frac{E_p}{M_R}} \right)^2}} + \frac{1 - \frac{1}{\sqrt{1 + \left(\frac{D}{a} \right)^2}}}{E_p} \right] \quad (\text{Eq. 4})$$

Where d_0 = deflection at the pavement surface (inches), adjusted to a standard temperature of 68° F

P = contact pressure under the loading plate (psi)

a = load plate radius (inches)

D = actual pavement structure thickness (inches)

M_R = subgrade resilient modulus (psi)

E_p = effective modulus of the pavement structure (psi)

Once E_p was determined, SN_{eff} could be calculated:

$$SN_{eff} = (0.0045) (D) (E_p)^{0.33} \quad (\text{Eq. 5})$$

Where SN_{eff} = effective structural number

D = total thickness of the pavement structure above the subgrade (inches)

E_p = effective modulus of the pavement structure above the subgrade (psi)

To accommodate the large quantity of data, the researchers developed a spreadsheet to calculate M_R , E_p , and SN_{eff} for each test section. Table 10 presents the statistics of these structural parameters.

Table 10. Structural Parameter Statistics for SPS-9B

Section	Date	M_R (psi)				E_p (psi)				SN_{eff}
		Average	Maximum	Minimum	COV (%)	Average	Maximum	Minimum	COV (%)	
04A901	1998	35,139	55,370	24,515	29.7	498,636	614,634	452,228	8.7	3.81
	1999	32,559	52,153	21,523	34.7	440,233	551,078	238,315	17.6	3.66
	2002	36,825	70,533	21,267	43.3	497,738	636,591	394,578	14.3	3.68
	2005	30,277	47,701	20,761	28.9	564,082	701,365	267,296	21.4	3.86
04A902	1994	40,516	59,080	30,069	20.9	257,499	330,556	130,614	26.3	2.64
	1995	31,850	48,152	25,516	19.0	192,128	389,925	50,390	66.1	1.93
	1998	30,504	38,197	24,257	11.8	134,876	292,195	40,179	72.1	1.67
	1999	27,665	32,782	23,529	11.3	125,552	294,307	44,668	69.8	1.71
	2002	32,725	43,584	25,824	14.8	125,464	222,999	89,133	36.0	2.13
	2005	29,577	35,283	24,127	10.9	145,526	275,853	79,105	54.2	2.15
040902	1994	30,656	33,680	27,636	7.1	230,124	262,850	186,866	11.2	2.90
	1995	28,014	30,615	26,402	4.7	104,787	168,434	68,446	30.2	2.16
	1998	29,626	34,155	24,129	15.1	60,127	80,121	42,441	23.6	1.80
	1999	28,619	34,478	23,468	13.2	61,886	83,857	48,393	21.5	1.83
	2002	34,678	53,887	26,363	23.0	108,332	144,199	84,104	19.4	2.31
	2005	29,191	33,535	25,061	9.9	112,618	193,695	66,031	38.1	2.21
04A903	1994	25,904	29,923	22,054	7.5	271,533	341,231	179,841	17.3	2.97
	1995	21,064	26,043	18,395	10.5	149,606	250,362	69,093	36.7	2.22
	1998	19,955	29,331	17,671	17.2	96,673	255,403	45,201	60.5	1.91
	1999	23,162	25,683	19,536	8.7	77,267	225,921	44,419	67.7	1.75
	2002	23,782	27,304	20,858	9.1	124,220	212,588	93,600	27.6	2.24
	2005	19,865	27,846	17,357	14.4	74,964	145,494	52,234	36.4	1.83
040903	1994	22,921	24,088	20,983	3.9	169,272	239,053	110,939	27.1	2.34
	1995	21,925	24,546	20,400	5.0	64,789	76,239	53,040	10.9	1.84
	1998	21,482	23,119	20,157	4.7	49,969	57,621	44,267	7.9	1.71
	1999	21,704	23,367	19,867	4.9	48,929	54,584	43,339	7.8	1.69
	2002	23,567	25,026	22,239	4.5	98,316	114,552	86,155	8.1	2.14
	2005	20,401	22,458	18,600	5.8	66,207	73,640	58,682	7.4	1.88

Section 04A901 had an M_R of 35 ksi in 1998, but M_R had decreased by 20 percent at the last round of testing in 2005. E_p increased from 498 ksi at the first round of testing in 1998 to 564 ksi in 2005. Section 04A901 showed little variation in SN_{eff} over time. Sections 04A902 and 040902 contained 1 inch and $\frac{3}{4}$ inch of Superpave Level I mix, respectively. In both sections, E_p and SN_{eff} showed a declining trend over time. Similar trends can also be observed in the replicate sections of 04A903 and 040903.

BACKCALCULATION USING EVERCALC SOFTWARE

The researchers also processed the FWD data using the backcalculation software Evercalc, which was developed by the Washington State Department of Transportation. One set of FWD data at each station was selected for backcalculation using the representative thickness of each test section obtained from the LTPP database to determine M_R of each layer. Table 11 shows the seed value and modulus range used for backcalculation. The pavement structure was first assumed to be a four-layer system: asphalt concrete, aggregate base, subgrade, and bedrock. However, after running several initial analyses, researchers found that the base layer was not producing reasonable moduli values. Consequently, instead of calculating each individual layer modulus, researchers combined the base layer with the subgrade layer and repeated the backcalculation analysis. This approach produced more reasonable moduli values.

Table 11. Backcalculation Seed Value and Modulus Range

Layer	Seed Modulus (ksi)	Poisson's Ratio	Minimum Modulus (ksi)	Maximum Modulus (ksi)
Asphalt concrete	400	0.35	100	2100
Aggregate base	25	0.3	10	150
Subgrade	15	0.4	5	50

Table 12 provides the statistics on the backcalculated moduli for the test sections. (The information in Table 12 is also shown graphically in Figures 8 and 9.) In general, backcalculated AC modulus decreased as pavement age increased, potentially caused by the progression of pavement distresses over time. Except in Section 04A901, there is a significant trend in AC moduli decreasing over time. In the case of 04A902, the AC moduli decreased after the first round of testing, and the values bounced back at the last round of testing. The values also bounced back in Section 040902, but in the second to last round of testing. The resulting trend coincides with other parameters discussed in the previous section. A similar decreasing trend can also be observed in the subgrade moduli among all the test sections. This type of decreasing trend in subgrade modulus did not occur using the AASHTO backcalculation procedure, which showed uniform subgrade modulus over time. The discrepancy could be caused by the assumption used in the Evercalc analysis, which combines the base and subgrade layers into one layer. If the subgrade fines penetrate into the base layer, the base modulus will weaken with time, and thus the combined subgrade (subgrade and base) modulus will decrease. In general, Sections 04A901, 04A902,

and 040902 have higher subgrade modulus values than Sections 04A903 and 040903. This finding is in agreement with the results of the AASHTO analysis procedure.

Table 12. Backcalculation Moduli Statistics for SPS-9B Test Sections

Section	Date	Backcalculated AC Modulus (ksi)	Backcalculated Subgrade Modulus (ksi)	Root-Mean Square Error (%)
04A901	1998	2100.0	37.9	4.56
	1999	1501.6	34.4	3.74
	2002	600.2	32.2	4.61
	2005	1550.3	30.6	1.68
04A902	1994	748.9	50.0	29.84
	1995	375.7	34.0	13.24
	1998	281.7	29.5	11.91
	1999	274.0	23.7	8.31
	2002	144.9	20.4	18.87
	2005	195.6	27.2	17.78
040902	1994	1033.1	37.8	12.92
	1995	463.1	28.2	11.29
	1998	293.4	25.1	13.7
	1999	276.9	20.6	12.96
	2002	235.0	28.9	22.61
	2005	166.6	25.7	14.43
04A903	1994	1254.8	28.5	3.52
	1995	412.7	20.1	1.12
	1998	353.4	16.9	4.02
	1999	237.8	15.6	13.71
	2002	193.8	14.1	13.13
	2005	309.0	11.4	16.59
040903	1994	684.7	24.5	2.6
	1995	197.3	16	10.64
	1998	198.8	15.6	11.04
	1999	190	13.4	15.56
	2002	177.8	12.4	16.67
	2005	234.6	12.4	16.99

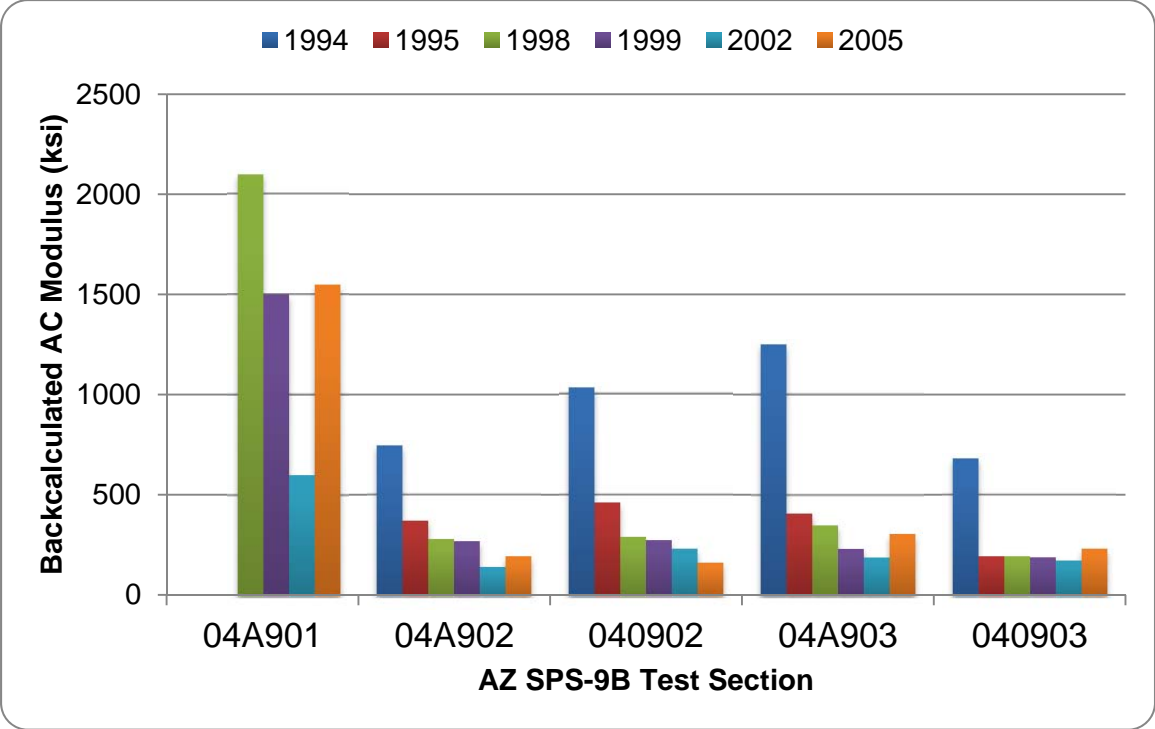


Figure 8. Backcalculated AC Modulus by Test Section (Evercalc Method)

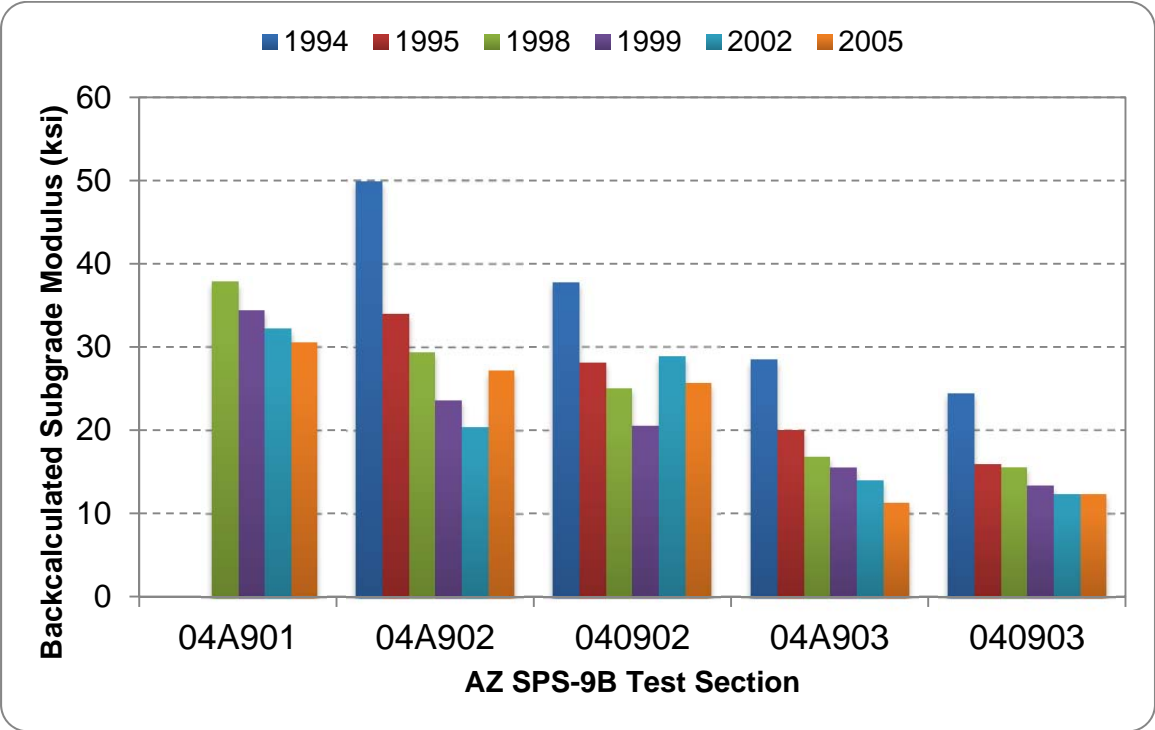


Figure 9. Backcalculated Subgrade Resilient Modulus by Test Section (Evercalc Method)

KEY FINDINGS FROM THE SPS-9B DEFLECTION ANALYSIS

The average maximum deflection increased in every SPS-9B test section except Section 04A901 between the first round of deflection testing in 1994 and the last round of testing in 2005. This may be due to weakening over time of the subgrade, the pavement structure above the subgrade, or both.

A clear declining trend in the average subgrade resilient modulus can be observed in Sections 04A901, 04A902, and 04A903 between the first round of testing and the last. There was little or no change in Sections 040902 and 040903. The decline in subgrade modulus could be due to a gradual increase and leveling off of the subgrade moisture content after construction.

Using the backcalculation procedure outlined in the *AASHTO Guide for Design of Pavement Structures* (1993), researchers observed the following regarding M_R , E_p , and SN_{eff} of the test sections:

- The trend in average E_p over time varied significantly across the sections. Section 04A901, the agency standard mix, showed an increasing trend between the first round of testing in 1994 and the last round in 2005. Sections 04A902 and 040902 showed reductions in average E_p of 51 percent and 43 percent, respectively, between the first round of testing and the last. Sections 04A903 and 040903 showed an even more significant drop in average E_p (decreases of 72 percent and 61 percent, respectively).
- The average backcalculated SN_{eff} declined in all but one of the test sections between 1995 and 2005, presumably due to damage from traffic loading. In Section 04A901, the average backcalculated SN_{eff} did not decrease, but rather increased slightly.
- Section 04A901 had the highest initial SN_{eff} value (3.81) among the test sections. Sections 040902 and 04A903 had similar initial SN_{eff} values of 2.90 and 2.97, respectively. Section 040903 had the lowest initial SN_{eff} at 2.34. At the last round of testing, the backcalculated SN_{eff} in Sections 04A902 and 040902 had declined to a similar level (2.2), and the replicate sections 04A903 and 040903 also showed similar behavior (each had a SN_{eff} of 1.8).
- Using the industrial standard backcalculation software Evercalc yielded the following results for subgrade resilient modulus and AC modulus:
 - In all sections, the backcalculated AC modulus declined between the first round of testing and the last.
 - In all sections, the backcalculated subgrade resilient modulus shows a declining trend over time, which does not agree with the results of the backcalculation analysis using the AASHTO procedure. This is likely due to the combination of the subgrade and base layers into one layer in the Evercalc analysis. If intermixing between the base and subgrade layers occurred, the base would weaken and the overall combined subgrade modulus could

decrease. In general, Sections 04A901, 04A902, and 040902 had higher subgrade moduli than Sections 04A903 and 040903.

CHAPTER 3. SPS-9B DISTRESS ANALYSIS

This chapter includes analyses and results from evaluating distress data collected from the SPS-9B site using LTPP manual survey techniques (Miller and Bellinger 2003). Surface distress provides powerful information regarding the nature and extent of pavement deterioration, which can be used to quantify performance trends as well as to investigate how design features affect service life.

All five of the flexible SPS-9B test sections were constructed consecutively and exposed to the same traffic loading, climate, and subgrade conditions. This allows for direct comparisons between layer configurations and design features without the confounding effects introduced by different in situ conditions.

AC DISTRESS TYPES

Surface deterioration is composed of multiple distress types. Definitions of each type follow (Huang 1993):

- **Fatigue cracking:** A series of interconnecting cracks caused by repeated traffic loading. Cracking initiates at the bottom of the asphalt layer where tensile stress is highest under the wheel load. With repeated loading, the cracks propagate to the surface.
- **Longitudinal wheelpath cracking:** Cracking parallel to the centerline occurring in the wheelpath. This cracking can be the early stages of fatigue cracking or can initiate from construction-related issues such as paving seams and segregation of the mix during paving. In the latter case, cracking is typically very straight (no meandering).
- **Longitudinal non-wheelpath cracking:** Cracking parallel to the centerline occurring outside the wheelpath. This cracking is not load-related and can initiate from paving seams or where mix segregation issues occurred during paving. Cracking can also be caused by tensile forces experienced during temperature changes. Pavements with oxidized or hardened asphalt are more prone to this type of cracking.
- **Transverse cracking:** Cracking that is predominantly perpendicular to the pavement centerline. This distress type initiates from tensile forces experienced during temperature changes. Pavements with oxidized or hardened asphalt are more prone to this type of cracking.
- **Block cracking:** Cracking that forms a block pattern and divides the surface into approximately rectangular pieces. This distress type initiates from tensile forces experienced during temperature changes. This type of distress indicates that the asphalt concrete has significantly oxidized or hardened.
- **Raveling:** Wearing away of the surface caused by dislodging of aggregate particles and loss of asphalt binder. Raveling is caused by moisture stripping and asphalt hardening.

- **Bleeding:** Excessive bituminous binder on the surface that can lead to loss of surface texture or a shiny, glass-like, reflective surface. Bleeding is a result of high asphalt content or low air void content in the mix.
- **Rutting:** A surface depression in the wheelpaths. Rutting can result from consolidation or lateral movement of material due to traffic loads. It can also signify plastic movement of the asphalt mix because of inadequate compaction, excessive asphalt, or a binder that is too soft given the climatic conditions.

The distress types defined above can be grouped into two general categories based on cause or failure mechanism: structural and environmental factors. Table 13 summarizes the flexible pavement distress types and their associated failure mechanisms.

Table 13. Flexible Pavement Distress Types and Failure Mechanisms

Distress Type	Failure Mechanism	
	Traffic/Loading Related	Climate/Materials Related
Fatigue cracking	X	
Longitudinal wheelpath cracking	X	
Longitudinal non-wheelpath cracking		X
Transverse cracking		X
Block cracking		X
Raveling		X
Bleeding		X
Rutting	X	X

RESEARCH APPROACH

Investigators began their analysis with a review of all distress data collected at each test section to identify suspect or inconsistent information. The analysis team used photos and distress maps to verify quantities reported in the database. Because of the subjective nature of the data collection technique (raters must select distress type and severity based on a set of rules), variation is expected in distress data. The SPS-9B data set was well within the acceptable range of variability.

Distress data collected for LTPP purposes are reported at three severity levels: low, moderate, and high. Inconsistencies between severity levels within a distress type create one of the largest sources of variability in distress data (Rada et al. 1999). In addition, conducting analyses on three separate severity levels for each distress type becomes increasingly complex, with results that are difficult to interpret. To reduce variability and to consolidate the information for analyses, the researchers summed the quantities from the three severity levels into one composite value.

As shown in Table 13, pavement deterioration (when not directly attributable to mix problems or construction deficiencies) can be attributed to structural or environmental factors. Structural factors are the result of traffic loading relative to the structural capacity of the pavement section. Environmental factors represent the influence of climate on pavement deterioration. Therefore, structural and environmental indices were developed to focus the analyses on overall structural and environmental damage, which are more consistent and provide a better avenue for comparison, rather than on individual types of distress, which vary from section to section and year to year.

The structural damage index consists of those distresses generally manifesting from the portion of the pavement that experiences loading (i.e., wheelpaths). Therefore, the structural damage index was presented as the percentage of wheelpath damage and included fatigue and longitudinal wheelpath cracking. To normalize fatigue and longitudinal cracking, the structural damage index took the form of the following expression:

$$S = \frac{F + 1ft \times C_{lwp}}{2W_{wp} L_s} \quad (\text{Eq. 6})$$

Where S = structural damage index

F = area of fatigue (ft²)

C_{lwp} = length of longitudinal wheelpath cracking (ft)

W_{wp} = width of wheelpath = 3.28 (ft)

L_s = length of test section (ft)

The environmental damage index is a composite of distresses that generally result from climatic effects. The entire pavement surface is subject to environmental distress; therefore, the environmental damage index was characterized as the percentage of total pavement area damaged. Typically, transverse cracking, longitudinal cracking (outside of the wheelpaths), and block cracking are specific to environmental damage. To normalize the environmental distress for the total area, the environmental damage index was expressed as:

$$E = \frac{B}{A_{tot}} + \frac{C_{nwp}}{L_s} + \frac{C_t}{L_s} \quad (\text{Eq. 7})$$

Where E = environmental damage index
 B = area of block cracking (ft²)
 C_{nwp} = length of non-wheelpath cracking (ft)
 C_t = length of transverse cracking (ft)
 A_{tot} = total area of test section (ft²)
 L_s = length of test section (ft)

Although the structural and environmental distress factors clearly affected the SPS-9B project's structural and functional service life, rutting, patching, and other surface defects (such as potholes, bleeding, and raveling) also affected performance. Rutting data reported in this study were generated using a 6-ft straightedge reference (Simpson 2001).

The experimental design of the SPS-9B project allowed for replicate data collection (Sections 040902 and 040903 are paired with Sections 04A902 and 04A903, respectively). However, since Sections 040902 and 04A902 received a slurry seal treatment in 2002, the researchers made comparisons using distress data collected in March and April 2002 (before the treatment) to eliminate any confounding effects from the slurry seal application.

OVERALL PERFORMANCE TREND OBSERVATIONS

While gathering pavement distress data, researchers became aware of a few significant trends affecting the overall pavement performance of the project. These observations were clearly driving issues for this project and were intrinsically important pieces of the distress performance.

Sections 040903 and 04A903 exhibited raveling in the wheelpaths in 2006. All test sections, with the exception of 04A901, experienced pumping between 1998 and 2006. Sections 040902 and 04A902 received a slurry seal in 2002 and were the only test sections to receive any major maintenance treatment. The Superpave sections that did not receive the slurry seal (040903 and 04A903) had large quantities of high-severity fatigue cracking and experienced raveling.

Figure 10 shows the structural damage trends for each section, and Figure 11 shows the environmental damage trends. The performance trends are relatively consistent and within the expected range of variation. The drop in structural damage after May 2002 for Sections 040902 and 04A902 indicates that the slurry seal masked the underlying deterioration. The drop in environmental damage in 2006 was due to fatigue cracking spreading to non-wheelpath areas that were previously rated as longitudinal and transverse cracking.

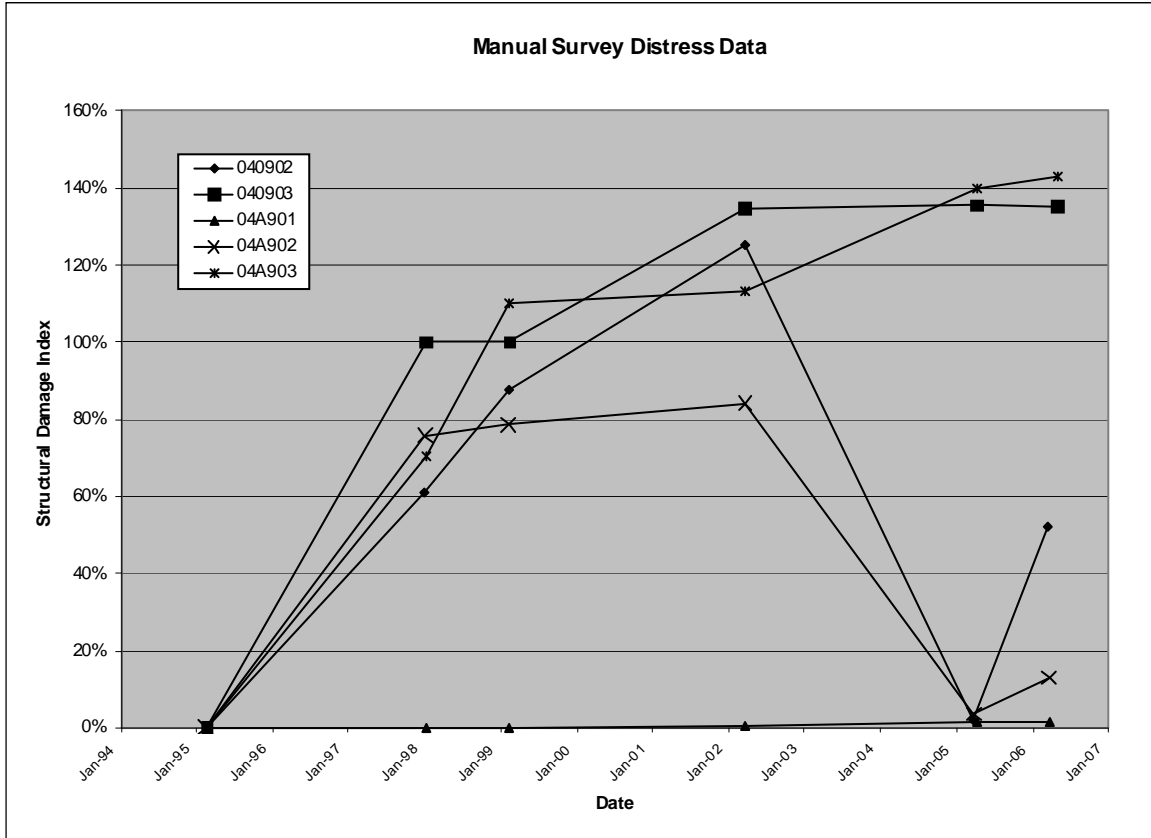


Figure 10. Structural Damage Trends for SPS-9B Test Sections

The Superpave sections contained a higher percentage of asphalt cement, which typically produces higher resistance to fatigue cracking. However, all Superpave sections showed a rapid accumulation of structurally related damage at early stages of the pavement life, approximately three years after construction. The accumulation typically slowed in later years.

Compared with the rest of the SPS-9B project, Section 04A901 exhibited significantly smaller amounts of structural and environmental damage accumulation, as shown in Figures 10 and 11. The pavement structure for Section 04A901 used the standard agency mix, which was used over a larger area extending beyond the test section limits.

The Superpave sections accumulated fatigue much earlier than the agency mix section (04A901). Factors that may have contributed to the rapid deterioration of the Superpave mixes include:

- The traffic loads on the pavement required a Superpave Level 2 mix design. However, only a Level 1 mix design was permitted due to the lack of equipment and testing protocols (Nichols Consulting Engineers 1997).

- During paving, the Superpave mixtures seemed to be susceptible to segregation, which was attributed to the coarseness of the mixture and to a paver problem. This resulted in random areas of significant surface voids (Nichols Consulting Engineers 1997).
- The Superpave mix design did not include any modifiers or anti-oxidizing agents (Nichols Consulting Engineers 1997).
- There may have been unforeseen construction issues due to the shorter lengths of the Superpave test sections and lack of contractor experience in constructing pavements using Superpave mixtures.

In 2002, a slurry seal was applied to Sections 040902 and 04A902. As shown in Figure 10, the slurry seal did improve the surface characteristics of the road. It appears to have had a significant effect on Section 04A902, based on a comparison of the structural distress three years after initial construction with the distress three years after the slurry seal. However, the data may be misleading because the sections experienced significantly decreased traffic loads after 2001 due to increased security over the Hoover Dam (see Table 8). Accounting for the reduced traffic loads, Section 040902 actually experienced nearly the same amount of structural damage three years after the slurry seal as it had three years after initial construction. This is most likely due to reflective cracking from prior damage. Though the slurry seal improved the road surface, the seal was applied after cracking was present, which was too late to be effective as a preventive maintenance treatment. The purpose of such an application is to slow crack initiation by reducing oxidation and weathering. Oxidation of the asphalt binder increases the brittleness of the binder and promotes raveling and cracking. Slurry seals do not increase the structural capacity of the pavement and are not thick enough to prevent existing cracks from reflecting through the treatment. If cracks are present in the existing pavement, a slurry seal will quickly reflect this cracking, thereby diminishing the expected resistance to oxidation and weathering.

Timing of surface applications is critical to the effectiveness of the treatments. Figure 10 shows that all Superpave sections already had a significant amount of cracking in 1998. Applying the slurry seal when there is not much cracking and the cracks are low in severity may result in slower deterioration and improved effectiveness of the treatment.

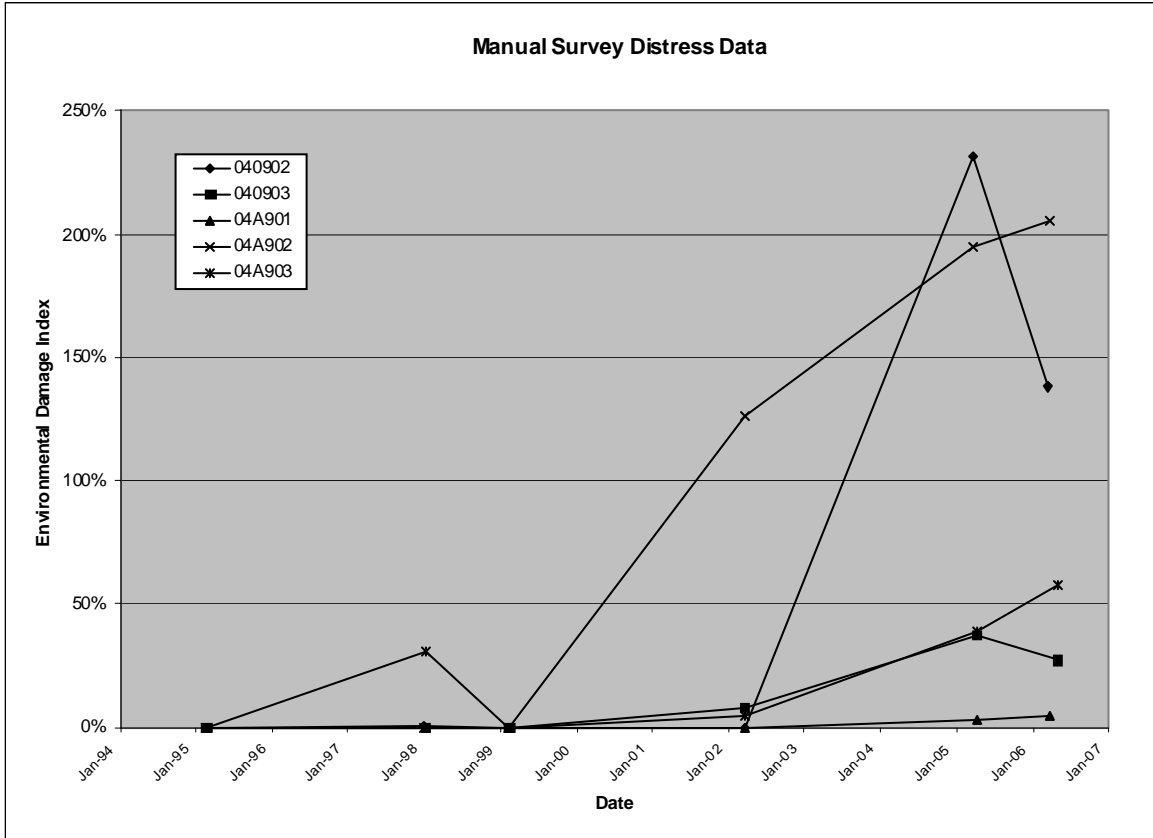


Figure 11. Environmental Damage Trends for SPS-9B Test Sections

As noted above, the performance trends for environmental damage are relatively consistent and within the expected range of variation (see Figure 11). Section 04A902 experienced the most environmental damage. The slurry seal applied in 2002 did not appear to have a significant impact on the performance of the Superpave sections (04A902 and 040902). Although slight decreases were somewhat discernible for surveys within a year of the slurry seal, environmental distresses clearly increased in magnitude approximately three years after the slurry seal was applied. There is no clear indication that the slurry seal provided any abatement in environmental distress.

As previously mentioned, Sections 040902 and 040903 are replicate sections; however, 040902 received a slurry seal treatment in 2002. Figures 10 and 11 show a noticeable difference in the performance trends of these replicates. Section 040902 has significantly less structural damage than Section 040903, but it also has significantly more environmental damage. The slurry seal treatment and the subjective nature of distress surveys most likely account for this discrepancy. Prior to receiving the slurry seal in 2002, Section 040902 had high-severity fatigue cracking throughout the entire section. When the slurry seal was applied, it masked the distress. In 2006, there was a significant amount of longitudinal cracking along the border of the inner wheelpath, which was most likely the beginning stages of fatigue cracking (structural distress) reflecting through the pavement. However, the longitudinal cracking was located

along the border of the wheelpath, and the surveyor rated the distress as non-wheelpath cracking (environmental distress). In 2006, Section 040903 showed high-severity distress cracking throughout the section and also contained a significant amount of moderately severe block cracking near the beginning of the section.

Performance Comparisons

The researchers conducted in-depth analyses and comparisons of all the SPS-9B test sections. Figure 12 summarizes the structural damage index and pavement structure for each section; Figure 13 summarizes the environmental damage index and pavement structure. Both damage indices are based on the data collected in March and April 2002 (before slurry seal application).

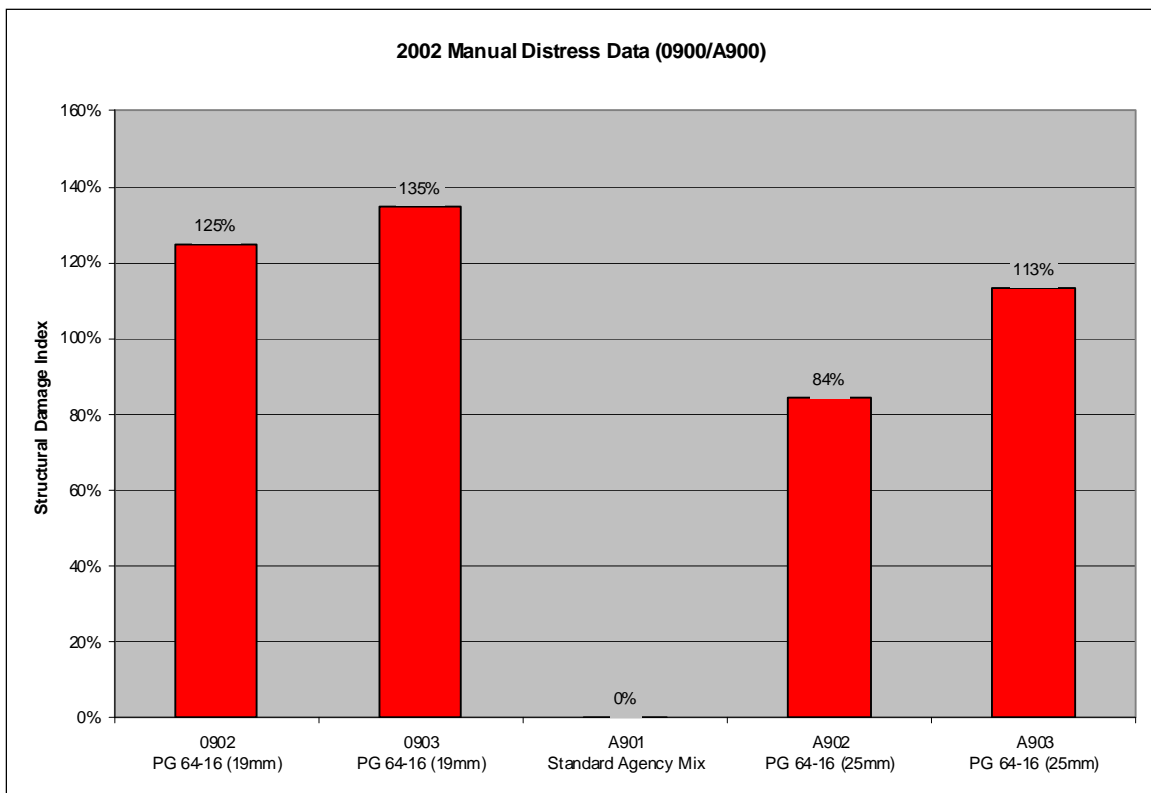


Figure 12. Structural Damage Index Summary

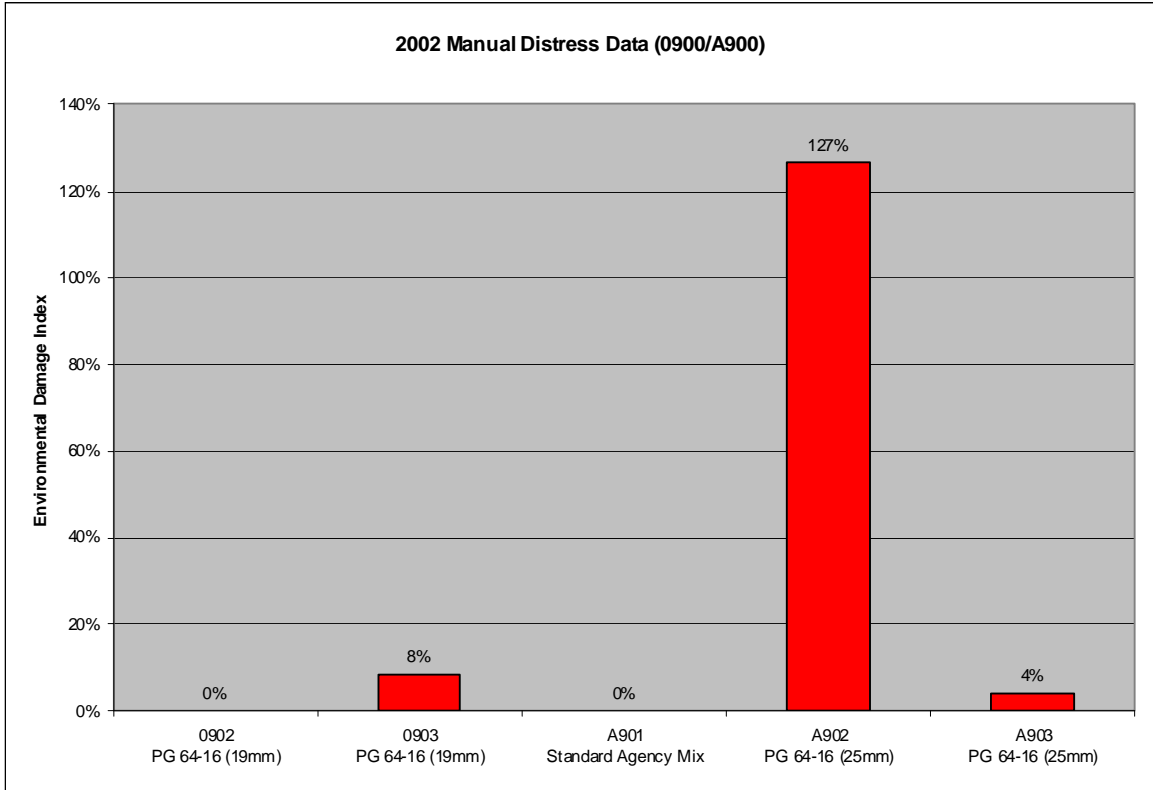


Figure 13. Environmental Damage Index Summary

Figure 14 summarizes the amount of rutting in each section as of March or April 2002. The Superpave sections experienced higher amounts of rutting than the agency mix section (04A901). Comparing the performance of the Superpave mixes, Sections 04A902 and 04A903 (25-mm gradation) performed slightly better than Sections 040902 and 040903 (19-mm gradation). However, all sections exhibited less than 9 mm of rutting after over seven years in service, which is well below the level required to trigger improvements in most pavement management systems. Therefore, rutting was not the driving factor in the overall condition of the pavement.

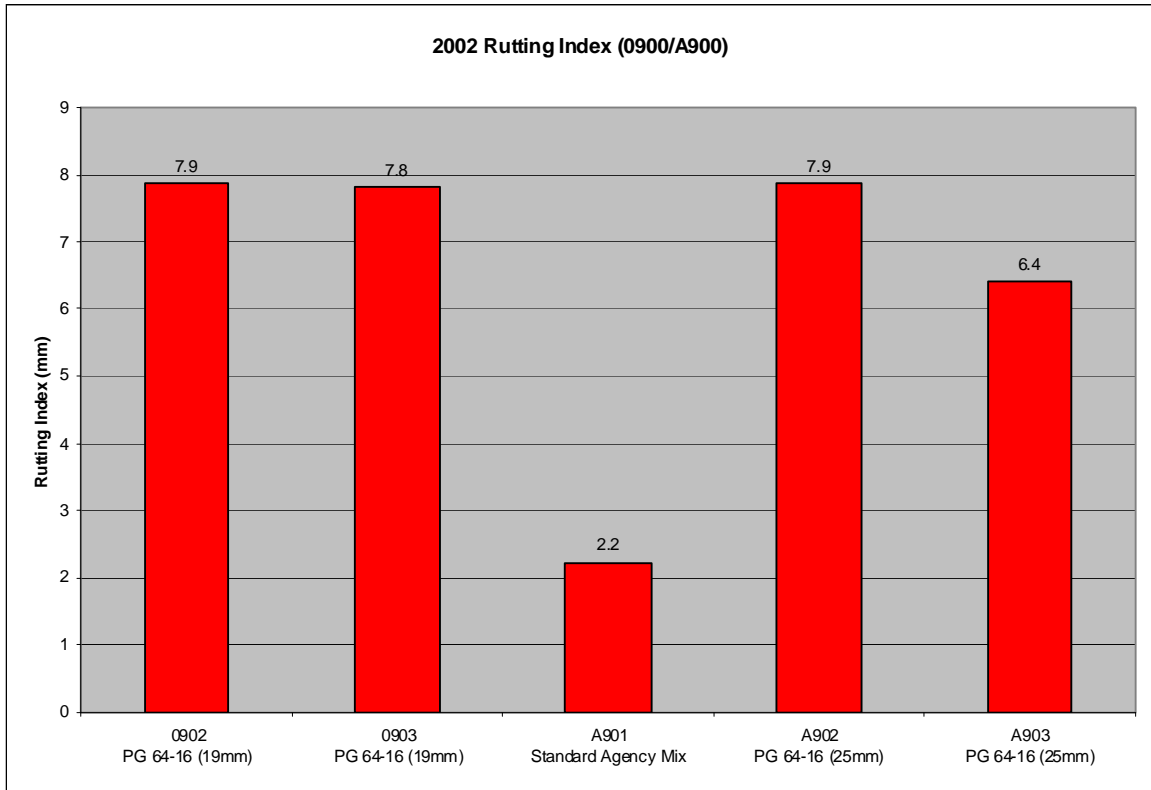


Figure 14. Rutting Index Summary

Following is a synopsis of the key findings for each section, including overall pavement performance, structural deterioration, environmental deterioration, rutting, and other unique circumstances.

Section 040902 (Superpave Level 1 Mix, 19-mm Gradation)

Section 040902 is similar to its replicate, 040903, but 040902 received a slurry seal in 2002. This slurry seal masked distress and promoted raveling resistance. This section exhibited premature structural failure and experienced the highest amount of environmental damage. This section experienced the most rapid increase in environmental distress among all the sections; this occurred from 2002 to 2005. The researchers attribute this section's decrease in environmental distress after 2005 to fatigue cracking spreading outside the wheelpath into existing environmental cracking. This caused cracks that were rated as environmental cracking in 2005 to be rated as fatigue cracking in 2006.

Section 040903 (Superpave Level 1 Mix, 19-mm Gradation)

Section 040903 is a replicate of 040902, but unlike 040902, it did not receive any maintenance during the monitoring period. Like 040902, 040903 experienced premature structural deterioration. In fact, this section accumulated the most structural damage and the most severe rutting of all the test sections. However, unlike its counterpart, it experienced significantly less environmental damage (the least of any

section except the agency mix, 04A901). This section also experienced pavement raveling in 2005 and 2006.

Section 04A901 (Standard Agency Mix, 19-mm Gradation)

The standard agency mix design performed significantly better than all the Superpave sections. Both structural and environmental deterioration on this section were well below the average for the SPS-9B project. Unlike the Superpave sections, this section did not experience pumping, and the amount of rutting was minimal.

Section 04A902 (Superpave Level 1 Mix, 25-mm Gradation)

This section exhibited premature structural and environmental deterioration. Section 04A902 experienced the largest amount of environmental distress of all the test sections. This section is similar to its replicate, 04A903, but 04A902 received a slurry seal in 2002. This slurry seal masked distress and promoted raveling resistance. However, this section experienced slightly less structural damage and significantly more environmental damage than its counterpart, 04A903.

Section 04A903 (Superpave Level 1 Mix, 25-mm Gradation)

Section 04A903 developed the most structural damage of all the test sections. This section is similar to its replicate, 04A902, but it did not receive any maintenance throughout the monitoring period. This section experienced slightly more structural damage and significantly less environmental damage than its counterpart, 04A902. This section also experienced pavement raveling in 2006.

KEY FINDINGS FROM THE SPS-9B DISTRESS ANALYSIS

The distress data captured at the SPS-9B project provide valuable insight into pavement performance, design, management, and construction. Highlights from the SPS-9B distress analysis follow:

- Two of the sections received a slurry seal coat in 2002. This masked the distress that developed early in the pavement life, but did not otherwise provide a significant improvement in environmental cracking. Replicates that did not receive the slurry seal experienced higher amounts of raveling.
- All Superpave sections experienced premature structural deterioration, showing significant growth in fatigue and longitudinal cracking within three years after construction (and in some cases earlier).
- The Superpave mix designs did not include any modifiers or anti-stripping agents, which may have contributed to their premature failure.
- Construction quality can play a major role in performance. All Superpave sections experienced segregation during construction that was attributed to the coarseness of the mix and to a paver problem. Segregation was occurring in the windrow during construction and resulted in random areas of significant surface voids. Additionally, kickback paddles of the paver appeared to be

worn, resulting in a segregated area in the middle of each pass. ADOT observed the mat from the Superpave mixtures to be very rich and “bony.” However, after three months of traffic the mat appeared less bony and rich, and segregation did not seem to be a problem. Other factors that may have contributed to the Superpave sections’ performance were the shorter lengths of the Superpave sections and a possible lack of contractor experience in constructing pavements using Superpave mixes as compared to the agency standard mix.

- All sections except for 04A902 had reasonable patterns of environmental distress growth, with a clear increase in magnitude approximately 10 years after construction.
- Sections constructed with Superpave mixes exhibited the largest accumulations of structural deterioration.
- Superpave sections with a 19-mm gradation performed slightly worse in terms of structural damage than those with a 25-mm gradation after seven years. However, this performance difference diminished after 11 years.
- All sections performed well with regard to rut resistance. In most sections, rutting would not have triggered a rehabilitation event.
- All Superpave sections experienced pumping by 1998.

CHAPTER 4. SPS-9B ROUGHNESS ANALYSIS

This chapter characterizes the surface roughness of the SPS-9B test sections throughout their service life and links the observations to records of pavement distress and its development. Investigators collected road profile measurements at the site about once per year starting with the winter after the site was opened to traffic. This study analyzed the profiles in detail by calculating their roughness values, examining the spatial distribution of roughness within them, viewing them with post-processing filters, and examining their spectral properties. These analyses provided details about the roughness characteristics of the road and provided a basis for quantifying and explaining the changes in roughness with time.

PROFILE DATA SYNCHRONIZATION

Profile data were collected from the entire Arizona SPS-9B site on 10 dates between 1994 and 2006 (see Table 14). Each visit took place during a visit to the SPS-1 site at the same location. (Note that the visit numbers in Table 14 correspond to visit numbers referenced in a companion report about the SPS-1 site, and that some visits to the SPS-1 site did not produce any profile measurements on SPS-9B test sections.) Raw profile data were available for all 10 visits. Each visit produced a minimum of seven repeat profile measurements.

Table 14. Profile Measurement Visits to the SPS-9B Site

Visit	Date	Time	Repeats	Section				
				04A901	040902	04A902	040903	04A903
01	Jan. 27, 1994	—	9					
02	Feb 27, 1995	12:45	9					
03	Jan. 23, 1997	09:54-12:50	9					
04	Apr. 8, 1998	13:50-15:31	7					
05	Dec. 4, 1998	10:40-12:16	7					
06	Nov. 17, 1999	09:26-11:06	7					
07	Dec. 19, 2000	11:26-13:31	9					
09	Feb. 20, 2002	10:41-14:25	9					
11	March 9, 2004	16:18-16:40	9					
11	March 10, 2004	11:29-13:34	9					
13	March 27, 2006	12:43-16:12	9					

DATA EXTRACTION

Researchers extracted profiles of individual test sections directly from the raw measurements for two reasons. First, profiles were collected in visits 03 through 09 at a 0.98-inch sample interval and in visits 11 and 13 at a sample interval of about 0.77 inches. These data appeared in the database after the application of an 11.8-inch moving average and decimation to a sample interval of 5.91 inches. The raw

data contained the more detailed profiles. Second, this study depended on consistency of the profile starting and ending points with the construction layout and consistency of the section limits with time. In particular, a previous quality check revealed that some profiles were shifted (Evans and Eltahan 2000).

In visits 02 through 07, 09, 11, and 13, researchers collected measurements from Sections 04A901, 040902, and 04A902 within long profiles that also included SPS-1 test sections. Sections 040903 and 04A903 were typically covered in a subsequent set of runs on the same date. The exception was visit 11, when Sections 040903 and 04A903 were measured on the previous day.

The raw data were used to synchronize all of the profiles to each other through their entire history. Profiles were synchronized using (1) the site layout from the construction report, (2) event markers in the raw profiles from the start and end of each section, and (3) automated searching for the longitudinal offset between repeat measurements.

CROSS CORRELATION

Searching for the longitudinal offset between repeat profile measurements that provides the best agreement between them is a helpful way to refine their synchronization. This can be done by inspecting filtered profile plots, but it is very time consuming. Visual assessment is also somewhat subjective when two profiles do not agree well, which is often the case when measurements are made several years apart. In this study, investigators used an automated procedure rather than visual inspection to find the longitudinal offset between measurements.

In this procedure, which is based on a customized version of cross correlation (Karamihas 2004), a basis measurement is designated that is considered to have the correct longitudinal positioning. A candidate profile is then searched for the longitudinal offset that provides the highest cross correlation to the basis measurement. A high level of cross correlation requires a good match of profile shape, the location of isolated rough spots, and overall roughness level. Therefore, the correlation level is often only high when the two measurements are synchronized. When the optimal offset is found, a profile is extracted from the candidate measurement with the proper overall length and endpoint positions. For the rest of this discussion, this process will be referred to as *automated synchronization*.

For this application, investigators performed cross correlation after the International Roughness Index (IRI) filter was applied to the profiles rather than using the unfiltered profiles. This helped assign the proper weighting to relevant profile features. In particular, it increased the weighting of short-wavelength roughness that may be linked to pavement distress. This enhanced the effectiveness of the automated synchronization procedure. The long-wavelength content within the IRI output helped ensure that the longitudinal positioning was nearly correct, and the short-wavelength content allowed investigators to leverage profile features at isolated rough spots to fine-tune the positioning.

SYNCHRONIZATION

To extract profiles of individual test sections from the raw measurements, investigators:

1. Established a basis measurement for each section using data from visit 06. This was done using the event markers from a raw measurement. The first repeat measurement of each section was used for this purpose. Visit 06 was selected because it included event markers near the expected locations in each test section. Each section was assumed to begin at the appropriate event marker and continue for 500 ft.
2. Automatically synchronized the other eight repeats from visit 06 to the basis set.
3. Automatically synchronized the measurements from the previous visit to the current basis set.
4. Designated the previous visit as the current visit.
5. Replaced the basis set with a new set of synchronized measurements from the first repeat of the current visit.
6. Repeated steps 3 through 5 for each visit from visit 05 to visit 01.

Visits 07 through 13 were also synchronized using steps 3 through 6, but going forward in time.

DATA QUALITY SCREENING

Investigators performed data quality screening to select five repeat profile measurements from each visit to each section. From the group of available runs, investigators selected the five measurements that exhibited the best agreement with each other. In this case, agreement between any two profile measurements was judged by cross correlating them after applying the IRI filter (Karamihas 2004). In this method, the IRI filter is applied to the profiles, and then the output signals are compared rather than the overall index. High correlation by this method requires that the overall roughness as well as the details of the profile shape that affect the IRI agree. The IRI filter was applied before correlation in this case for several reasons:

- Direct correlation of unfiltered profiles places a premium on very long-wavelength content, but ignores much of the contribution of short-wavelength content.
- Correlation of IRI filter output emphasizes profile features in (approximate) proportion to their effect on the overall roughness.
- Correlation of IRI filter output provides a good trade-off between emphasizing localized rough features at distressed areas in the pavement and placing too much weight on the very short-duration, narrow features (spikes) that are not likely to agree between measurements. This is because the IRI filter amplifies short-wavelength content, but attenuates macrotexture, megatexture, and spikes.

- A relationship has been demonstrated between the cross correlation level of IRI filter output and the expected agreement in overall IRI (Karamihas 2004).

Note: This method was performed with a special provision for correcting modest longitudinal distance measurement errors.

Each comparison between profiles produced a single value that summarized their level of agreement. When nine repeat profile measurements were available, they produced 36 correlation values. Any subgroup of five measurements could be summarized by averaging the relevant 10 correlation values. Researchers selected the subgroup that produced the highest average and excluded the other repeats from most of the analyses discussed in the rest of this report. Since the number of available profiles ranged from six to nine, the number of measurements that were excluded ranged from one to four. Tables 15 through 19 list the selected repeats for each visit to each section and the composite correlation level they produced.

Table 15. Selected Repeats, Section 04A901

Visit	Repeat Numbers					Composite Correlation
02	2	3	5	7	8	0.845
03	2	3	4	7	8	0.887
04	1	2	3	4	6	0.847
05	1	2	3	6	7	0.876
06	1	2	4	5	6	0.891
07	1	2	7	8	9	0.910
09	1	2	3	4	5	0.909
11	1	3	4	7	9	0.813
13	2	4	6	7	8	0.848

Table 16. Selected Repeats, Section 040902

Visit	Repeat Numbers					Composite Correlation
01	1	2	5	7	8	0.894
02	2	3	4	5	9	0.936
03	3	4	6	7	8	0.919
04	1	2	3	6	7	0.852
05	1	2	3	5	7	0.923
06	2	3	5	6	7	0.940
07	2	4	5	7	8	0.941
09	3	4	5	8	9	0.928
11	2	3	7	8	9	0.949
13	2	3	4	5	9	0.949

Table 17. Selected Repeats, Section 04A902

Visit	Repeat Numbers					Composite Correlation
01	2	4	6	7	8	0.897
02	3	5	6	7	8	0.953
03	4	5	7	8	9	0.934
04	1	2	5	6	7	0.939
05	1	2	3	5	7	0.955
06	2	3	5	6	7	0.956
07	1	3	6	7	9	0.970
09	2	3	4	7	8	0.957
11	1	3	5	7	8	0.969
13	2	3	5	7	9	0.970

Table 18. Selected Repeats, Section 040903

Visit	Repeat Numbers					Composite Correlation
03	5	6	7	8	9	0.946
04	1	2	3	4	5	0.877
05	1	2	3	4	7	0.928
06	2	3	4	5	6	0.949
07	3	4	6	8	9	0.952
09	1	2	4	5	6	0.955
11	3	4	5	6	9	0.759
13	1	2	5	6	7	0.756

Table 19. Selected Repeats, Section 04A903

Visit	Repeat Numbers					Composite Correlation
03	1	5	7	8	9	0.963
04	2	4	5	6	7	0.916
05	2	3	4	5	7	0.932
06	1	2	3	6	7	0.949
07	1	3	5	6	7	0.964
09	1	4	5	7	8	0.939
11	2	3	4	5	8	0.891
13	4	5	6	8	9	0.896

The process described above for selecting five repeat measurements from a larger group is similar to the practice within LTPP except that it is based on composite agreement in profile rather than the overall index value. The correlation levels listed in Tables 15 through 19 provide an appraisal of the agreement between profile measurements for each visit of each section. When two profiles produce a correlation

level above 0.82, their IRI values are expected to agree within 10 percent most (95 percent) of the time. Above this threshold, the agreement between profiles is usually acceptable for studying the influence of distresses on profile. When two profiles produce a correlation level above 0.92, they are expected to agree within 5 percent most of the time. Above this threshold, the agreement between profiles is good. Correlation above 0.92 often depends on consistent lateral tracking of the profiler, and may be very difficult to achieve on highly distressed surfaces. Note that the IRI values provided in this report are the average of five observations, which tightens the tolerance even further.

Overall, the majority of the groups of measurements listed in Tables 15 through 19 exhibited good or better correlation, and most exhibited acceptable correlation. Any group of repeat measurements that produced a composite correlation level below 0.82 was investigated using filtered plots. These are discussed below:

- **Section 04A901, visit 11:** Correlation was diminished by sinusoidal chatter in the profiles.
- **Section 040903, visits 11 and 13:** Correlation was significantly diminished by a large number of narrow downward spikes in the profiles, particularly on the right side.

SUMMARY ROUGHNESS VALUES

Figures 15 through 19 show the left and right IRI values for each pavement section over its monitoring period. This includes up to 20 summary IRI values (two per visit over up to 10 visits). The figures show the IRI values versus time in years. In this case, “years” refers from the number of years between the measurement date and the date the site was opened to traffic, which was August 1, 1993. Fractions of a year are estimated to the nearest day.

To supplement the plots, the appendix to this report lists the IRI, Half-car Roughness Index (HRI), and Ride Number (RN) of each section for each visit. These roughness values are the average of the five repeat measurements selected in the data quality screening. These are not necessarily the same five repeat measurements selected for the LTPP database. The appendix also provides the standard deviation of IRI over the five repeat measurements. This helps identify erratic roughness values that result from transverse variations in profile caused by surface distresses.

Figures 15 through 19 provide a snapshot of the roughness history of each pavement section. The remainder of this chapter characterizes the profile content that made up the roughness and explains the profile features that contributed to roughness progression.

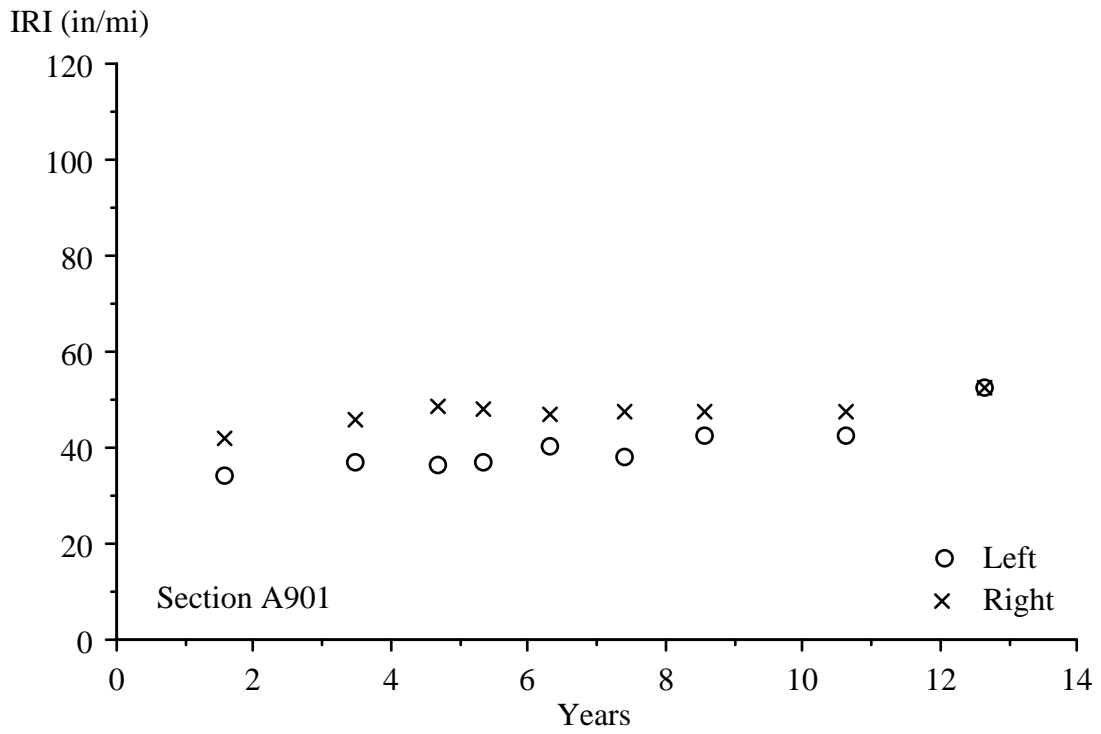


Figure 15. IRI Progression, Section 04A901

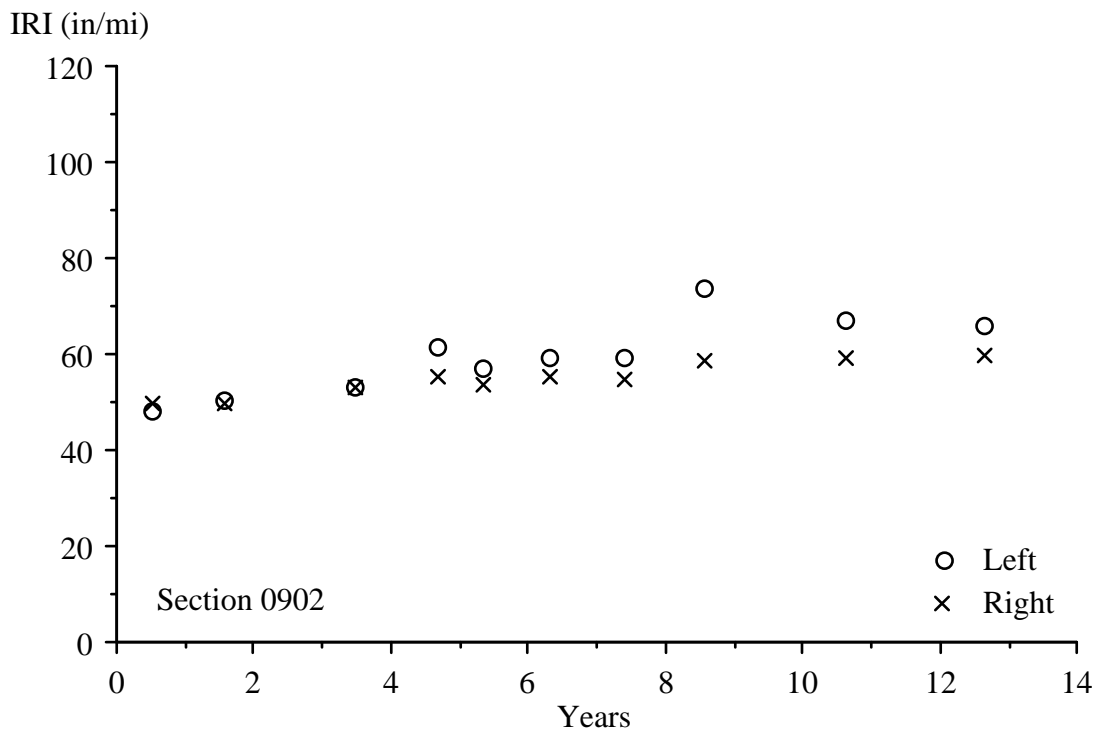


Figure 16. IRI Progression, Section 040902

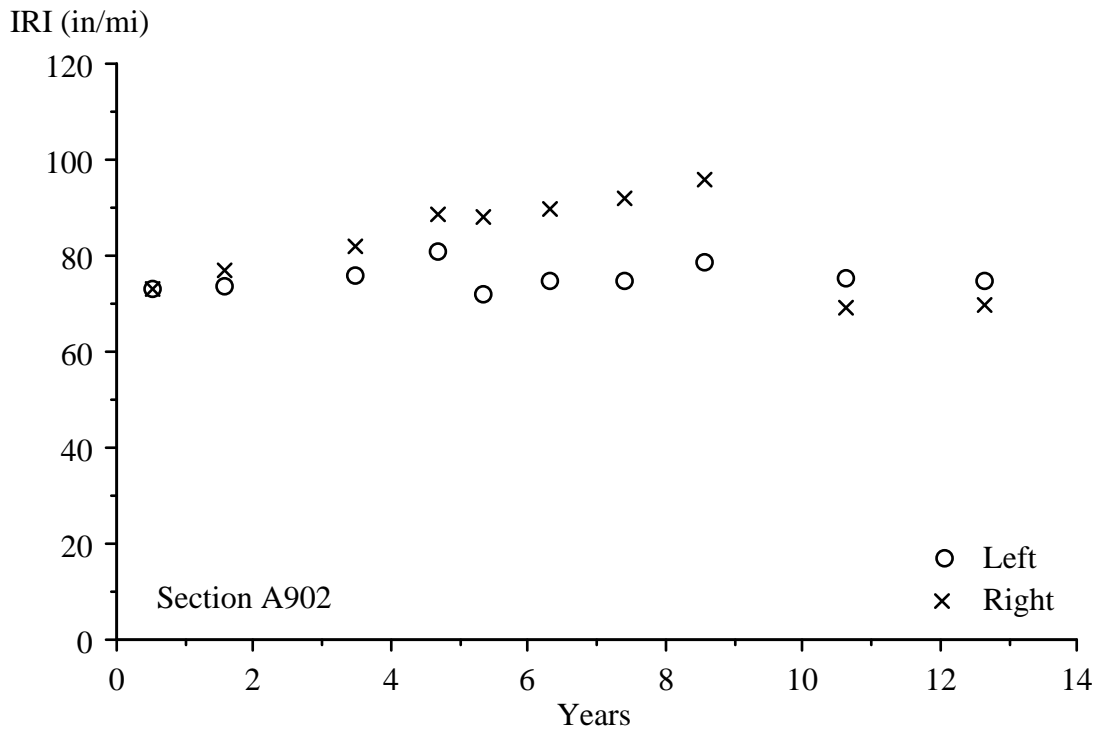


Figure 17. IRI Progression, Section 04A902

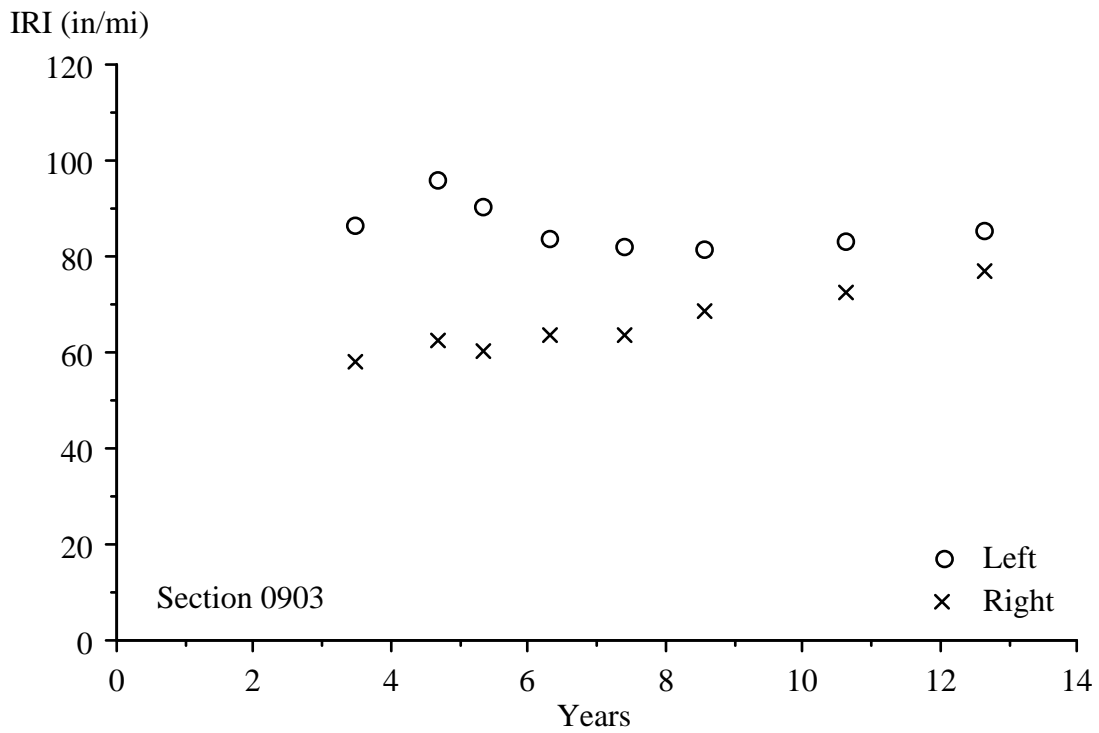


Figure 18. IRI Progression, Section 040903

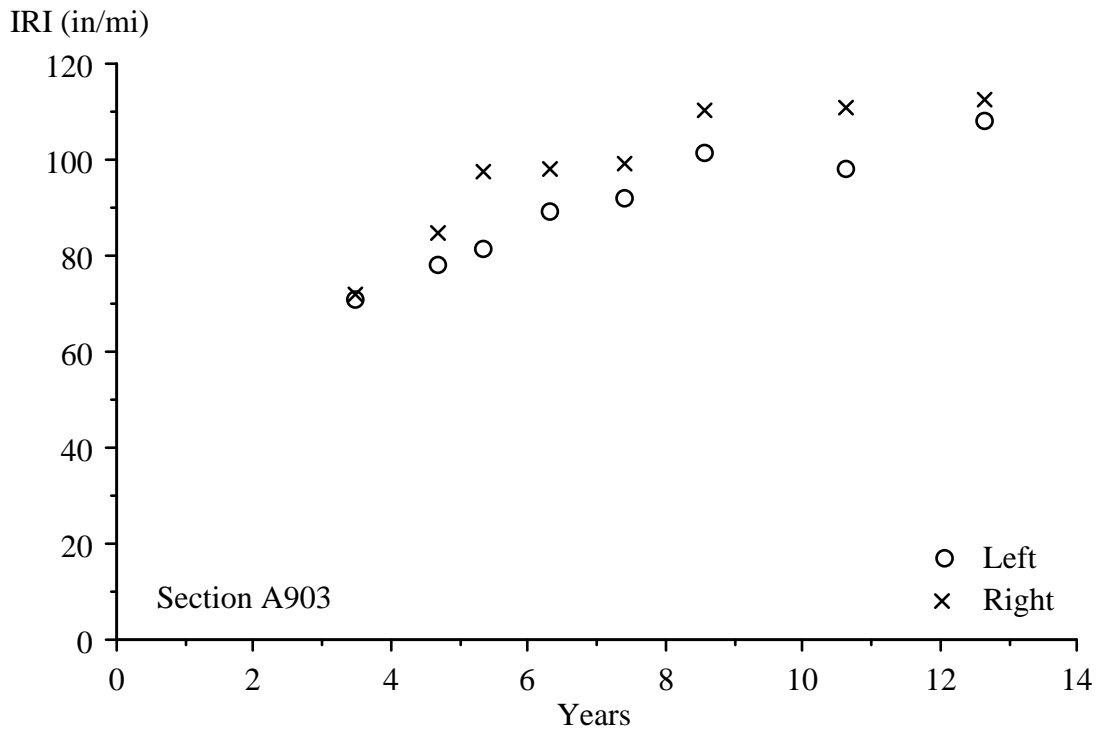


Figure 19. IRI Progression, Section 04A903

PROFILE ANALYSIS TOOLS

Investigators used various analysis techniques to study the profile characteristics of each pavement section and their change with time. These tools help study roughness, roughness distribution, and roughness progression of each test section, including concentrated roughness that may be linked to pavement distress. The discussion of each analysis and plotting method is rather brief; Sayers and Karamihas (1996b) provide more details about these methods.

Roughness Values

Investigators calculated left IRI, right IRI, Mean Roughness Index (MRI), HRI, and RN values. The appendix to this report provides the average value of each index for each visit of each section. The discussion of roughness in this analysis emphasizes the left and right IRI. Nevertheless, comparing the progression of HRI and RN to the MRI provides additional information about the type of roughness that is changing. For example, a low HRI value relative to MRI indicates roughness that exists on only one side of the lane. Further, aggressive degradation of RN without a commensurate growth in MRI signifies that the developing roughness is biased toward short-wavelength content.

Elevation Profile Plots

A simple way to learn about the type of roughness that exists within a profile is to view the trace. However, certain key details of the profile are often not as obvious in a raw profile trace as they may be after the profile is filtered. Three types of filtered plots were inspected for every visit of every section:

- Long wavelength: A profile smoothed with a base length of 25 ft and anti-smoothed with a base length of 125 ft.
- Medium wavelength: A profile smoothed with a base length of 5 ft and anti-smoothed with a base length of 25 ft.
- Short wavelength: A profile smoothed with a base length of 1 ft and anti-smoothed with a base length of 5 ft.

These filters were used to screen the profiles for changes with time and special features of interest. The terms “long,” “medium,” and “short” are relative, and in this case pertain to the relevant portions of the waveband that affects the IRI. The long-wavelength portion of the profile was typically very stable over time. However, the long-wavelength profile plots of every section changed somewhat between visits 09 and 11. This was not caused by a change in the surface characteristics of the section, but by a change in profiler make and the associated change in filtering practices.

The medium-wavelength plots provided a view of the features in a profile that were likely to have a strong effect on the IRI and may change with time. The short-wavelength elevation plots also typically progressed with time, but only affected the IRI through localized roughness or major changes in content with time. However, the short-wavelength elevation plots helped identify and track the progression of narrow dips and other short-duration features that may have been linked to distress.

Filtered profile plots also helped to characterize the effects of maintenance operations. For example, a slurry seal was applied to two of the sections in May 2002 (between visit 09 and 11). In most cases, this caused a complete change to the short-wavelength profile plots and a significant change to the medium-wavelength profile plots.

In addition to filtered plots, every profile was viewed in its raw form. This helped reveal noteworthy features that did not necessarily affect the IRI, but helped establish a link between surface distress and profile properties. Two examples of this were: (1) narrow downward spikes in the profiles caused by raveling, and (2) several densely spaced dips in the left profile on Section 04A901 caused by surface damage in the wheelpath.

Roughness Profile

A roughness profile provides a continuous report of road roughness using a given segment length (Sayers 1990). Instead of summarizing the roughness by providing the IRI for an entire pavement section, the roughness profile shows the details of how IRI varies with distance along the section. It does

this by using a sliding window to display the IRI of every possible segment of a given base length along the pavement.

A roughness profile displays the spatial distribution of roughness within a pavement section. As such, it can be used to distinguish road sections with uniform roughness from sections with roughness levels that change over their length. Further, the roughness profile can pinpoint locations with concentrated roughness and estimate the contribution of a given road disturbance to the overall IRI.

In this work, roughness profiles were generated and viewed using a base length of 25 ft. That means that every point in the plot shows the IRI of a 25-ft-long segment of road, starting 12.5 ft upstream and ending 12.5 ft downstream. Any location where a peak occurs in the roughness profile that is greater than or equal to 2.5 times the average IRI for the entire section is considered an area of *localized roughness*. All areas of localized roughness are discussed in the detailed observations by identifying them, listing their severity, and describing the underlying profile features that caused them.

Power Spectral Density Plots

A power spectral density (PSD) plot of an elevation profile shows the distribution of its content within each waveband. An elevation profile PSD is displayed as mean square elevation versus wave number, which is the inverse of wavelength. PSD plots were calculated from the slope profile rather than the elevation profile, which aided in the interpretation of the plots because the content of a slope PSD typically covers fewer orders of magnitude than an elevation PSD.

A PSD plot is generated by performing a Fourier transform on a profile (or in this case, a slope profile). The value of the PSD in each waveband is derived from the Fourier coefficients and represents the contribution to the overall mean square of the profile in that band.

The slope PSD plots provided a very useful breakdown of the content within a profile. In particular, the plots reveal (1) cases in which significant roughness is concentrated within a given waveband; (2) the type of content that dominates the profile (e.g., long, medium, or short wavelength); (3) the type of roughness that increases with time; and (4) the type of roughness that is stable with time.

For the SPS-9B project, the PSDs rarely provided much value beyond what was learned using filtered elevation plots and roughness profiles. However, any valuable observations that could be made from PSD plots are discussed in the following section.

Distress Surveys and Maintenance Records

Once the analysis and plotting were completed, all of the observations were compared to the manual distress surveys performed on each section. Manual distress survey results were available for each section on six dates over the monitoring history starting in February 1995. The surveys were performed using LTPP protocols by technicians certified to perform distress surveys. The surveys provided a means of relating profile features to known distresses.

Researchers also compared observations of changes in profile properties to maintenance records. In particular, crack sealing affected the presence and shape of narrow dips in one section, and the application of a slurry seal affected the short- and medium-wavelength content within the profiles on two sections.

DETAILED OBSERVATIONS

This section reports key observations from the roughness index progression, PSD plots, filtered elevation profile plots, roughness profiles, and distress surveys. In many cases, similar behavior was noted for multiple sections. These observations are repeated in each section where appropriate. However, changes in profile properties with time that were caused by changes in profiler make or model are not discussed here. These observations are summarized at the end of the report.

Section 04A901, Right Side

Roughness

The IRI increased steadily from 42 to 53 inches/mi over visits 02 through 13.

Elevation Profile Plots

The short-, medium-, and long-wavelength elevation profile plots were very consistent throughout the monitoring period, with the exception of the area from 360 to 430 ft from the start of the section. In this area, the medium-wavelength profile plots changed significantly with each visit. In all visits, a bump over 0.4 inches high appears from 360 to 410 ft from the start of the section. The transitions into and out of the bump became harsher (i.e., sharper) with time.

Roughness Profiles

Profiles changed very little with time over the first 360 ft of the section. In the last 140 ft of the section, the roughness increased aggressively with time, and by visit 13 the area centered 413 ft from the start of the section qualified as localized roughness. The localized roughness there was caused by the trailing end of the long bump, and had become a sharp slope break by visit 13.

Distress and Maintenance History

Very little distress was recorded for this section, even in later visits.

Section 04A901, Left Side

Roughness

The IRI increased steadily from 35 to 53 inches/mi over visits 02 through 13.

Elevation Profile Plots

The unfiltered elevation profile plots included two areas with strong periodic chatter about 250 to 280 ft and 440 to 465 ft from the start of the section in some repeat measurements from all visits. The chatter usually appeared as a series of narrow dips about 0.1 inch deep and 0.7 ft apart. (In many areas, the chatter approximated a sinusoid.) In visits 04 and 11, many of the repeat measurements included the chatter in the locations above, as well as most of the first half of the section. Figure 20 shows an example of the chatter (and its hit-or-miss nature) from visit 04.

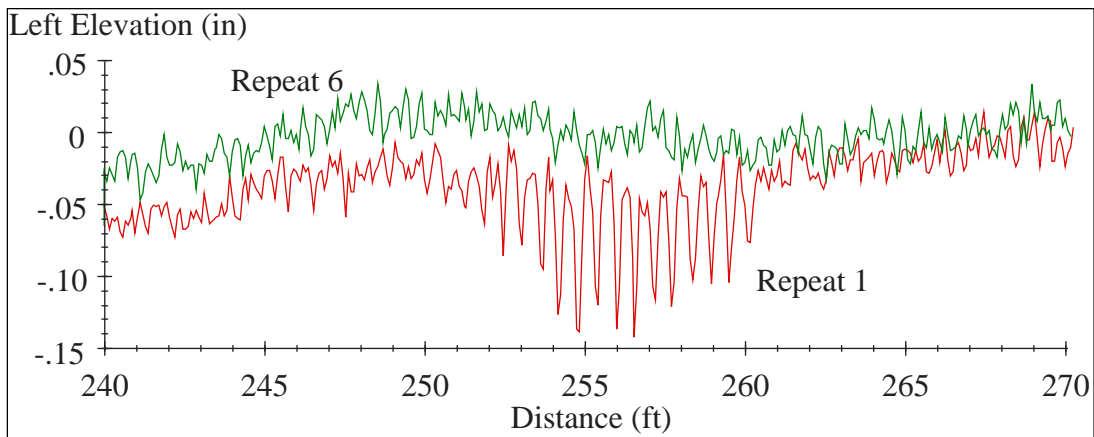


Figure 20. Periodic Chatter in Elevation Profiles from Section 04A901, Left Side

The later visits showed a bump in the profile from about 402 to 410 ft from the start of the section. It grew in severity with time, and was nearly 0.2 inches high by visit 13. In visit 13, unlike in other visits, this bump was preceded by another one that was equally severe.

Roughness Profiles

The roughness was very evenly distributed throughout the section in visits 02 through 05. The roughness of the first 380 ft of the section was consistent throughout the monitoring period. This indicates that the chatter observed in the profiles did not affect the IRI much. (If it had, the roughness in the first half of the section would have escalated in visits 04 and 11.)

All of the increase in roughness in the later visits took place in the last 120 ft of the section, and most of it was concentrated around 410 ft from the start of the section. This was caused almost entirely by the bumps mentioned above. By visit 13, an area of localized roughness was centered 410 ft from the start of the section, with a peak value of nearly 200 inches/mi in the roughness profile.

PSD Plots

All of the PSD plots included a peak at a wavelength of about 0.6 ft.

Distress and Maintenance History

Very little distress was recorded for this section, even in later visits. Nothing in the distress histories explains the bump that caused the localized roughness. A large transverse crack was noted in March 2006 that did appear in the visit 13 profiles as a bump about 44 ft from the section start, but it did not affect the IRI much.

The chatter in the profile corresponds to a narrow scuff that runs along the left wheelpath over most of the section and runs off to the edge near the end. It is present in the photos and appears as a long series of indents about a third of the width of the lane edge stripe. (See Figure 21.)



Figure 21. Pavement Scuff in the Left Wheelpath, Section 04A901

Section 040902, Right Side

Roughness

The IRI increased steadily from 50 to 60 inches/mi.

Elevation Profile Plots

Profiles were very consistent throughout visits 01 through 09, with the exception of some developing roughness in the medium-wavelength range. The elevation profiles in the medium- and short-

wavelength ranges changed significantly between visits 09 and 11, such that the shape and severity of most features was often totally different between visits. However, the elevation profiles were extremely consistent in all 10 repeat measurements from visits 11 and 13. In visits 11 and 13, the feature that stood out most was a bump 0.1 inch high and 6 ft wide from 78 to 84 ft from the start of the section. Three other small disturbances were found in the short-wavelength elevation profile plots 162, 208, and 451 ft from the start of the section.

Roughness Profiles

The roughness was distributed evenly across the section in visits 01 through 09, and the roughness profiles were fairly consistent across those visits. The visit 11 roughness profiles were significantly different from those of visit 09. Roughness profiles from visits 11 and 13 were very consistent with each other, and included one area of localized roughness and another area where localized roughness was developing. The first was at the bump 78 to 84 ft from the start of the section. This caused a peak in the roughness profile of about 210 inches/mi. The second rough area appeared about 450 ft from the start of the section, with a peak value of 120 inches/mi.

Distress and Maintenance History

A slurry seal coat was applied in May 2002. This accounts for the major change in medium- and short-wavelength content between visits 09 and 11. Nothing in the distress surveys explains the localized roughness found 78 to 84 ft and 450 ft from the start of the section. Distress surveys from April 2005 and March 2006 identified a significant number of cracks that did not appear to add roughness to the profiles.

Section 040902, Left Side

Roughness

The IRI generally followed an increasing trend from 48 inches/mi at visit 01 to 66 inches/mi at visit 13. An out-of-trend spike in roughness occurred at visit 09, with an IRI value of 74 inches/mi.

Elevation Profile Plots

No rough features stood out in the short-wavelength roughness plots in visits 01 through 06. In visit 07, a dip up to 0.4 inches deep and about 0.5 ft long appeared 213.5 ft from the start of the section. It was not present in any other visit. Visit 09 profiles included several shallow bumps that did not appear in profiles from visit 07 or 11. The medium- and short-wavelength elevation profile plots were very similar in all 10 repeats from visits 11 and 13, but those plots were very different from visit 09. In particular, the short-wavelength plots were much smoother in visits 11 and 13 than in visit 09.

Roughness Profiles

Roughness was distributed fairly evenly throughout the section in visits 01 through 07, except that the area from 160 to 260 ft from the start of the section was about twice as rough as the rest. The narrow

dip 213.5 ft from the start of the section was not severe enough to produce localized roughness. The shallow bumps and extra short-wavelength roughness in visit 09 caused it to be rougher than previous visits over the last three-quarters of the section. In visits 11 and 13, some areas of the section were rougher than others, but no localized roughness was found. The highest peak in the roughness profile was caused by a rise in pavement elevation of about 0.25 inches over 5 ft of pavement beginning about 61 ft from the start of the section.

Distress and Maintenance History

A slurry seal coat was applied in May 2002. This accounts for the major change in medium- and short-wavelength content between visits 09 and 11. Nothing in the distress surveys explains the narrow dip found in visit 07 or the shallow bumps found in visit 09.

Section 04A902, Right Side

Roughness

The IRI increased steadily from 73 to 96 inches/mi in visits 01 through 09, then diminished to about 69 to 70 inches/mi in visits 11 and 13.

Elevation Profile Plots

Profiles were somewhat consistent from visits 01 through 09. The profiles from visits 11 and 13 were very consistent with each other. However, in the short-wavelength range they were not at all similar to profiles from previous visits, and were markedly different in most locations in the medium-wavelength range.

Roughness Profiles

The profiles from visits 01 through 09 included severe localized roughness centered about 260 to 265 ft from the start of the section. This was caused by a sharp change in slope at the bottom of a long, deep dip (over 100 ft long and more than 1 inch deep). The dip included a high level of short-wavelength roughness at and near its lowest point. Overall, the dip caused a peak in the roughness profile of 240 to 280 inches/mi. In visits 11 and 13, the dip caused a much lower level of peak roughness (150 to 160 inches/mi).

The roughness profiles showed that the roughness progressed across most of the section in visits 01 through 09. The roughness profiles also showed that the roughness was not particularly evenly distributed along the section in visits 11 and 13, with higher roughness found 60 to 100 ft from the start of the section, about 410 ft from the start of the section, and at the bottom of the long dip described above.

Distress and Maintenance History

A slurry seal coat was applied in May 2002. This accounts for the change in medium- and short-wavelength content between visits 09 and 11. Crack sealing was performed on this section in May 2001, but no major changes occurred in the profiles.

Distress surveys from April 2005 and March 2006 show significant transverse cracking, but no strong effect (e.g., dips) was found in the profiles.

Section 04A902, Left Side

Roughness

The IRI ranged from 73 to 81 inches/mi without an increasing trend. The highest value occurred in visit 04.

Elevation Profile Plots

Profiles were somewhat consistent in visits 01 through 09. The most noteworthy feature of the profiles was a set of narrow dips that appeared 355 to 400 ft from the start of the section in visits 05 through 09. These dips were usually well repeated within a given visit, but they did not always appear in the same place in different visits.

The profiles from visits 11 and 13 were very consistent with each other. However, they were not at all similar in the short-wavelength range to profiles from previous visits, and were markedly different in most locations in the medium-wavelength range. The profiles from visits 11 and 13 included a bump about 0.25 inches high and 0.5 ft long that was 87.5 ft from the start of the section, and a bump 0.2 inches high that ranged from 406 to 414 ft from the start of the section. Neither of these features were found in previous visits.

Roughness Profiles

The profiles from visits 01 through 09 included localized roughness centered about 260 to 265 ft from the start of the section. This was caused by a sharp change in slope at the bottom of a long, deep dip (over 100 ft long and more than 1 inch deep). It caused a peak in the roughness profile of 170 to 230 inches/mi.

In visits 11 and 13, the two bumps described above caused peaks in the roughness profile of over 120 inches/mi, but they were not severe enough to be classified as localized roughness. The long dip that caused localized roughness in visits 01 through 09 was still present, but it was not as severe.

Distress and Maintenance History

A slurry seal coat was applied in May 2002. This accounts for the change in medium- and short-wavelength content between visits 09 and 11. Nothing in the distress surveys explains the two bumps

noted in visits 11 and 13. Crack sealing was performed on this section in May 2001, but no major changes occurred in the profiles.

Section 040903, Right Side

Roughness

The IRI increased steadily from 58 to 77 inches/mi from visits 03 through 13.

Elevation Profile Plots

Profiles were very consistent throughout visits 03 through 09, with the exception of some developing roughness in the medium-wavelength range. Profiles from visits 11 and 13 were also very similar to previous visits in the long- and medium-wavelength range, and somewhat similar in the short-wavelength range. However, unfiltered plots from visits 11 and 13 included a high density of narrow downward spikes up to 0.3 inches deep that appeared throughout the section. The spikes rarely appeared in the same location in more than one or two of the repeat measurements.

Roughness Profiles

The roughness was not particularly evenly distributed along the section, but no areas of localized roughness were found. The growth in roughness was not isolated to one area.

Distress and maintenance history: A very high level of distress was recorded in April 2005 and May 2006. This includes fatigue with water bleeding and pumping, and raveling along the entire right wheelpath. Cracking and raveling, which are confirmed by the photos, explain the narrow downward spikes dispersed throughout the profiles from visits 11 and 13.

Section 040903, Left Side

Roughness

The IRI followed an unusual trend with time. It was 87 inches/mi in visit 03, 96 inches/mi in visit 04, 91 inches/mi in visit 05, and 82 to 85 inches/mi over the rest of the visits.

Elevation Profile Plots

Profiles were fairly consistent across visits 03 through 05. Profile plots in the long-, medium-, and short-wavelength ranges were very consistent in visits 06 through 13. However, profiles from visits 11 and 13 included narrow downward spikes up to 0.5 inches deep that appeared throughout the section. The spikes often appeared in the same location in more than one of the repeat measurements. Fewer spikes appeared in the left side profiles than on the right, and the spikes that did appear often occurred in more than one repeat measurement. Figure 22 shows the density and shape of the spikes over 100 ft of the section in visit 13. In some locations, the spikes appear in only one repeat measurement of the five, but in others the spikes appear in multiple repeats.

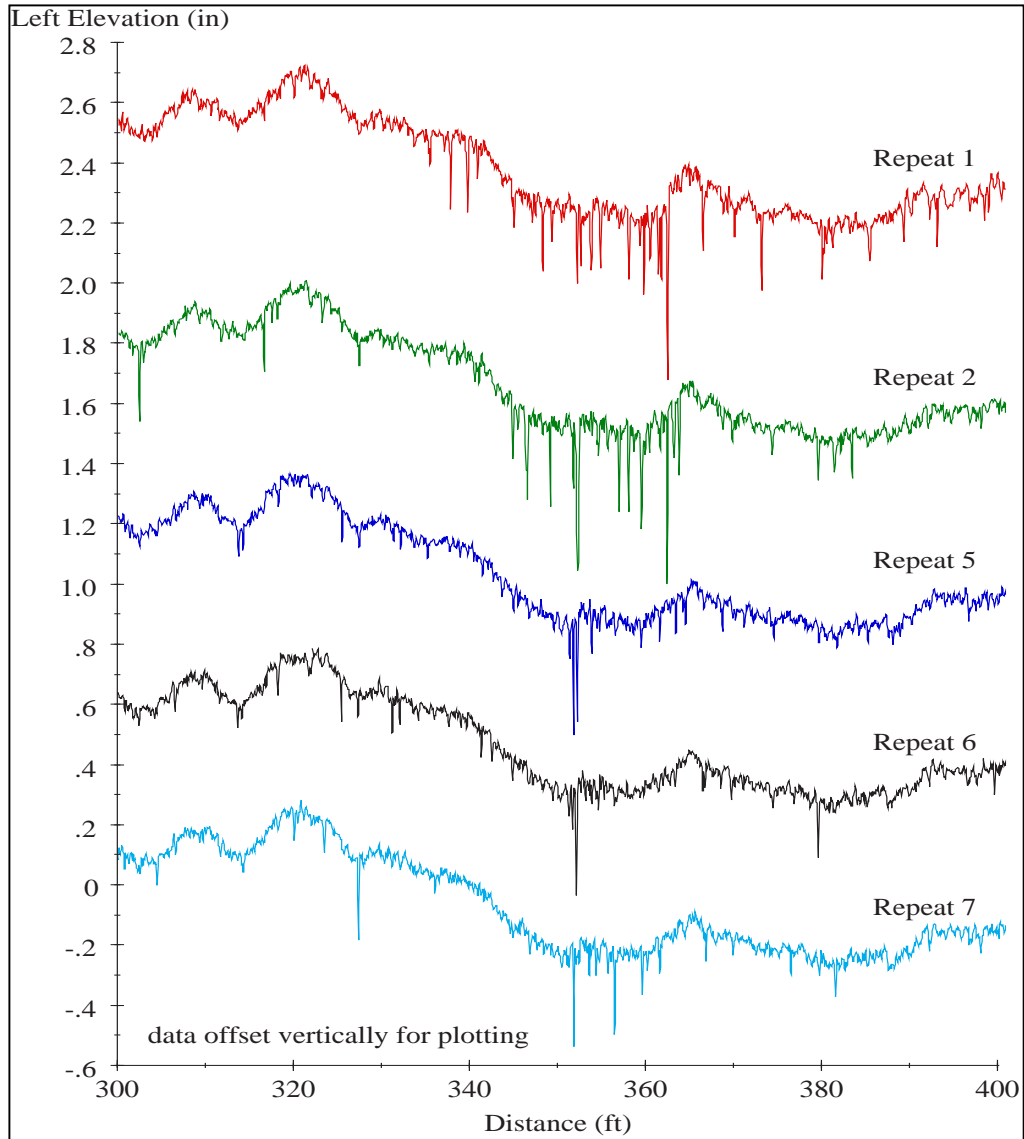


Figure 22. Narrow Downward Spikes in Elevation Profile, Section 040903, Visit 13

Roughness Profiles

The roughness was not particularly evenly distributed along the section; the middle third was the roughest. No areas of localized roughness were found. Although visits 03 through 05 were the roughest, the roughness profiles did not change much over the monitoring period.

PSD Plots

Significant content was isolated near a wavelength of 40 ft.

Distress and Maintenance History

A very high level of distress was recorded in April 2005 and May 2006. This includes fatigue with water bleeding and pumping, and raveling along the entire right wheelpath. Cracking and raveling, which are confirmed by the photos, explain the narrow downward spikes dispersed throughout the profiles from visits 11 and 13.

Section 04A903, Right Side

Roughness

The IRI increased from 72 inches/mi in visit 03 to 113 inches/mi in visit 13. In visits 05 through 07, the IRI held steady at 98 to 99 inches/mi, and in visits 09, 11, and 13, the IRI was stable at 111 to 113 inches/mi.

Elevation Profile Plots

Profiles did not change much over visits 05 through 07. Unfiltered profiles from visits 11 and 13 included several downward spikes throughout the length of the section that appeared in only one repeat measurement in some locations, and in up to three repeats in other locations. With the exception of the spikes, the profiles from visits 09, 11, and 13 were consistent with each other.

Roughness Profiles

Localized roughness was detected about 70 ft from the start of the section, which caused a peak in the roughness profile of 180 to 240 inches/mi over the monitoring period. The roughness was caused by a sharp change in slope about 60 ft from the start of the section at the bottom of a long dip.

In visits 03 through 13, the progression in roughness was very evenly distributed along the section (i.e., when roughness increased, it increased equally along the section). The roughness profiles from visits 11 and 13 were very similar to those from visit 09. This is because the spikes in the profiles from visits 11 and 13 were not numerous or severe enough to add significant roughness.

Distress and Maintenance History

A very high level of distress was recorded in April 2005 and May 2006. This includes fatigue with water bleeding and pumping as well as raveling along the entire right wheelpath. Cracking and raveling, which are confirmed by the photos, explain the narrow downward spikes dispersed throughout the profiles from visits 11 and 13.

Section 04A903, Left Side

Roughness

The IRI increased steadily from 71 inches/mi in visit 03 to 108 inches/mi in visit 13.

Elevation Profile Plots

The medium- and long-wavelength elevation plots were fairly consistent in visits 03 through 07. However, the short-wavelength elevation plots became rougher over time, with the greatest increase between visits 06 and 09.

The unfiltered elevation profile plots revealed several features that affected roughness. In visit 09, a dip less than 1 ft long and up to 0.5 inches deep appeared 45 ft from the start of the section. The dip was not detected in visit 11. It was detected in visit 13 in two of the five repeat measurements, where it was nearly an inch deep. A less severe dip also appeared 57 ft from the start of the section in two of the five repeat measurements from visit 09.

Profiles from visits 11 and 13 included several downward spikes throughout the length of the section that were rarely in the same location in more than one repeat measurement.

Roughness Profiles

No localized roughness was found in any visit, although the roughness was not particularly evenly distributed along the section. The growth in roughness was not confined to any particular area.

Distress and Maintenance History

A very high level of distress was recorded in April 2005 and May 2006. This includes fatigue with water bleeding and pumping as well as raveling along the entire left wheelpath. Cracking and raveling, which are confirmed by the photos, explain the narrow downward spikes dispersed throughout the profiles from visits 11 and 13. Nothing in the distress measurements explains the dip 45 ft from the start of the section.

SUMMARY

This section summarizes important observations from each section within the SPS-9B site. Several of the observations are common to more than one pavement section. In conjunction with the roughness progression plots (Figures 15 through 19), this summary provides the essential information about each pavement section. More detail on the profile properties as well as information about data handling and data quality control is provided in other chapters of this report.

A slurry seal coat was applied to Sections 040902 and 04A902 in May 2002. In both sections, the seal coat modified the short-wavelength content of the profiles significantly. Often, the net result was temporary smoothing of raveling and of narrow dips that appeared at cracks. In both sections, the medium-wavelength content of the profiles was also altered. This usually meant that high and low points within the medium-wavelength profile plots occurred in roughly the same places, but with altered shape and severity.

The slurry seal coat reduced the IRI in both sections. The change was largest on the right side of Section 04A902, where the IRI decreased by 27 inches/mi. The change occurred because the right-side profiles often included a higher level of narrow dips caused by cracking, which were smoothed out by the seal coat.

Placement of the seal coat also improved the relationship between the right and left profiles by eliminating narrow dips and uncorrelated short-wavelength content. This is demonstrated by the fact that the difference between the HRI and MRI decreased from 27 percent to 14 percent in Section 040902 and from 25 percent to 10 percent in Section 04A902.

Profiles from Sections 040903 and 04A903 in visits 11 and 13 included several downward spikes that often appeared in only one or two repeat measurements of each location. These were caused by cracking and raveling, which covered both wheelpaths; the spikes were more prevalent in the right wheelpath. The spikes did not affect the IRI significantly.

Significant raveling was also recorded in both sections from visit 09 onward, but the visit 09 profiles did not include the downward spikes. The explanation may be the change in profiler height sensor footprint between visits 09 and 11 (Perera and Kohn 2005). In visits 11 and 13, researchers used an International Cybernetics Corporation MDR 4086L3 profiler. This profiler's height sensor had a footprint about 1.5 mm in diameter. In visits 03 through 09, researchers used a K.J. Law Engineers T-6600 profiler, which had a height sensor with a footprint that was 38 mm wide and 6 mm long.

The change in profiler in late 2002 affected the long-wavelength content of the profiles on every test section. This is because the newer profiler used a high-pass filter that eliminated a little more of the profile content than the previous device. The change had no probable effect on the measurement of localized roughness or the study of narrow bumps and dips caused by distress. However, it did confound the study of the true effect of the slurry seal coat, since the device change and application of the seal coat both occurred between visits 09 and 11.

Another minor device effect within the profiles was peaks in the PSD plots with no pavement-related explanation. In visits 01 and 02 (measured by the K.J. Law DNC 690), most PSD plots from the left side included a strong peak at a wavelength of 2.5 ft. In visits 03 through 09 (measured by the K.J. Law T-6600), all profiles from the left and right sides included a peak in their spectral content at a wavelength somewhere between 0.35 and 0.65 ft and another at a wavelength of double the first.

Individual Test Sections

The summaries below provide the most important observations made about each test section. To help provide context for these summary statements, Figure 23 shows the range of left and right IRI for each section. Note that the highest IRI value for some of the sections did not occur in the final visit. (See the appendix or Figures 15 through 19.)

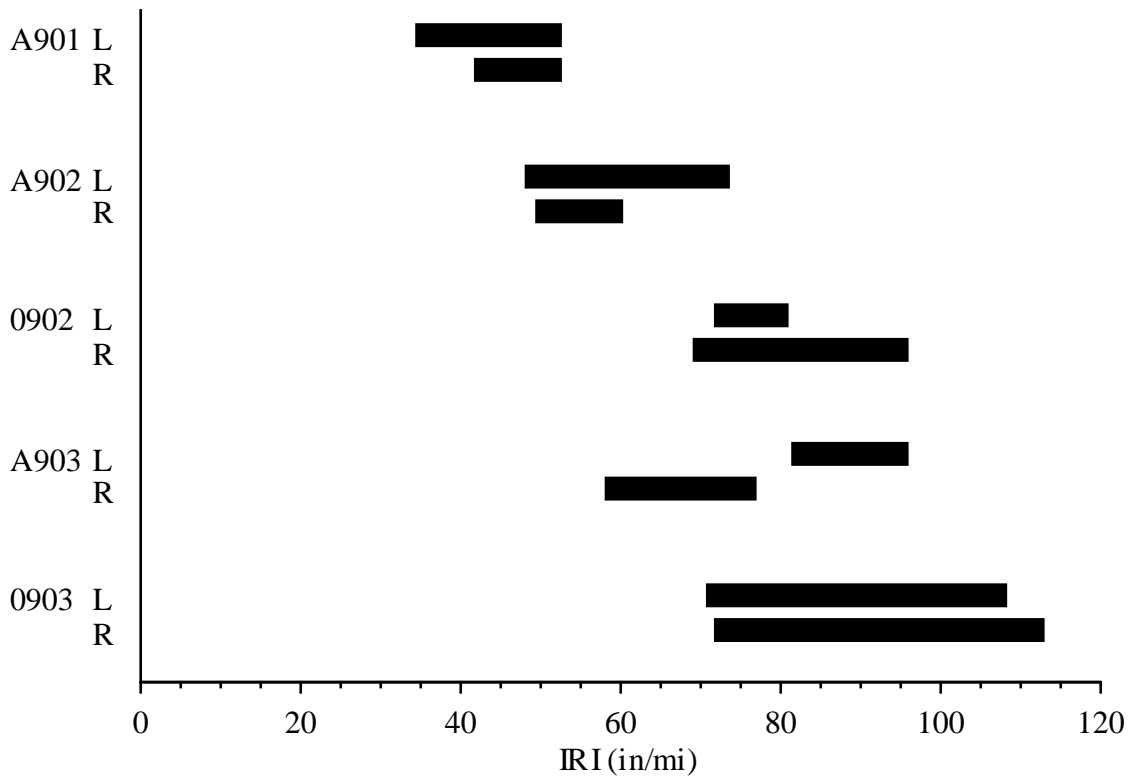


Figure 23. Summary of IRI Ranges

Section 04A901

The left side profiles in this section included two patches of sinusoidal chatter in all visits, and included chatter over the first half of the section in visits 04 and 11. This affected the look of the profiles

tremendously, but it did not affect the IRI much. A bump appeared about 400 ft from the start of the section that became rougher with time, causing localized roughness by visit 13.

Section 040902

The short- and medium-wavelength roughness in this section was altered by the application of a slurry seal coat in May 2002, which significantly reduced the roughness of the right side. Localized roughness was found on the right side in visits 11 and 13 at a bump 0.1 inch high from 78 to 84 ft from the start of the section. A severe narrow dip 0.5 ft long and 0.4 inch deep was found 213.5 ft from the start of the section in visit 07 only. No corresponding distress was noted.

Section 04A902

The short- and medium-wavelength roughness in this section was altered by the application of a slurry seal coat in May 2002, which significantly reduced the roughness of the right side. A long, deep dip from about 205 to 320 ft from the start of the section increased the roughness of the section significantly. The increase in roughness appeared on both sides, but it was much harsher in the right side profiles. The feature that affected the roughness most was the change in slope at the deepest part of the dip, and the short-wavelength roughness there. The dip registered a much lower level of concentrated roughness on the right side after the seal coat.

Section 040903

This section showed significant signs of fatigue over the entire pavement surface by the end of the monitoring period. The profiles from visits 11 and 13 included a large number of narrow downward spikes caused by cracking and raveling. The location and severity of the spikes was not well correlated between repeat measurements. No localized roughness was found in this section.

Section 04A903

This section showed significant signs of fatigue over the entire pavement surface by the end of the monitoring period. The profiles from visits 11 and 13 included a large number of narrow downward spikes caused by cracking and raveling. The location and severity of the spikes was not well correlated between repeat measurements. Localized roughness was detected about 70 ft from the start of the section because of a sharp change in slope at the bottom of a long dip centered 10 ft upstream.

CHAPTER 5. CONCLUSIONS AND RECOMMENDATIONS

ADOT initiated the SPS-9B project to study the relative performance of the Superpave mix designs for asphalt pavements compared to the agency standard mix design, which will provide a foundation for future design decisions. While it was found that the agency standard mix design had better performance in terms of both structural cracking and smoothness, it should be recognized that Superpave mix designs and construction practices have evolved over the past two decades. (In addition, site-specific conditions and construction issues may have negatively affected the performance of the Superpave mixes in this study.) Surface distress, deflection, and profile data were used as the basis for performance evaluation and were analyzed as part of the study.

The SPS-9B project offers a unique opportunity to directly compare performance of various mix designs while reducing the confounding effect of other variables such as traffic loading, climate, and subgrade conditions. Conclusions drawn from this comparison are based on one set of in situ conditions; observations from other climate or loading scenarios may differ from those in this report. Additionally, the Superpave traffic design and the segregation experienced during the construction of the Superpave sections may have significantly impacted performance, and the contribution of these factors could not be fully isolated in the analysis. Therefore, this study's findings may be unique to the conditions and construction of this site.

Despite these issues, the data captured at the project provide valuable insight into pavement performance, design, management, and construction. Following is a summary of lessons learned from the performance data collected at the SPS-9B site:

- Roughness and roughness progression alone cannot be used to represent the health of a test section. Several test sections did not exhibit changes in roughness in proportion to the amount of fatigue cracking, and sections that had clearly reached the end of their service lives did not necessarily have roughness values that would trigger a rehabilitation event.
- In 2002 two test sections received a slurry seal coat, which altered the profile features significantly and reduced the IRI values. The seal coat masked the distress that began early in the pavement life, but it did not otherwise significantly improve environmental cracking. Replicates that did not receive the slurry seal experienced higher amounts of raveling.
- Placement of the seal coat improved the relationship between the right- and left-side profiles by eliminating narrow dips and uncorrelated short-wavelength content.
- All Superpave sections experienced premature structural deterioration, showing significant growth in fatigue and longitudinal cracking within three years after construction and in some cases even earlier. Prompted by the overwhelming presence of fatigue, water bleeding, and pumping, staff from ADOT, FHWA, and Nichols Consulting Engineers conducted a field review of these sections in 1998. The initial conclusion was that the Superpave sections developed premature cracking due to stripping of the asphalt concrete (Sebaaly et al. 2001).

- The Superpave mix designs did not include any modifiers or anti-stripping agents, which may have contributed to their premature failure.
- Construction quality can play a major role in performance. All Superpave sections experienced segregation during construction that was attributed to the coarseness of the mix and to a paver problem. Other factors that may have contributed to the Superpave sections' performance included shorter-length Superpave sections and a possible lack of contractor experience with using Superpave mixes as compared to the agency standard mix.
- All sections except for 04A902 had reasonable patterns of environmental distress growth, with a clear increase in magnitude approximately 10 years after construction.
- Sections constructed with Superpave mixes exhibited the largest accumulations of structural deterioration.
- The agency standard mix (04A901) performed the best both in terms of structural cracking and smoothness.
- Superpave sections with a 19-mm gradation performed slightly worse in terms of structural damage than those with a 25-mm gradation after seven years, but this difference in performance diminished after 11 years.
- All sections performed well with regard to rut resistance. In most sections, rutting would not have triggered a rehabilitation event.
- All Superpave sections experienced pumping by 1998.
- A change in profiler equipment or profiler height sensor footprint can greatly affect roughness data. A profiler change during the test period may have disguised raveling.

Based on these findings, the research team makes the following recommendations:

- Site-specific conditions related to design traffic level and construction issues may have negatively influenced the performance of the test sections constructed with Superpave mixes. Therefore, it is important to investigate the performance of other Superpave mixes to obtain a better understanding of Superpave performance.
- The timing of maintenance treatments such as slurry seals should be studied further to determine the optimum timing to slow environmental deterioration of the pavement.
- Most of the pavement test sections appeared to have experienced top-down cracking, but this could not be confirmed. It is recommended that forensic analysis be performed at other locations throughout Arizona to learn about the factors contributing to top-down cracking.

REFERENCES

- American Association of State Highway and Transportation Officials (AASHTO). 1993. *AASHTO Guide for Design of Pavement Structures*. Washington, D.C.: American Association of State Highway and Transportation Officials.
- Evans, L. D. and A. Eltahan. 2000. *LTPP Profile Variability*. Publication FHWA-RD-00-113. McLean, VA: Federal Highway Administration.
- Huang, Y. H. 1993. *Pavement Analysis and Design*. Englewood Cliffs, NJ: Prentice-Hall.
- Karamihas, S. M. 2004. "Development of Cross Correlation for Objective Comparison of Profiles." *International Journal of Vehicle Design* 36(2/3): 173–193.
- Karamihas, S. M., T. D. Gillespie, and S. M. Riley. 1995. "Axle Tramp Contribution to the Dynamic Wheel Loads of a Heavy Truck." Proceedings of the 4th International Symposium on Heavy Vehicle Weights and Dimensions, Ann Arbor, MI. C. B. Winkler (ed.): 425–434.
- Kim, Y. R., B. Underwood, M. Sakhaei Far, N. Jackson, and J. Puccinelli. 2011. *LTPP Computed Parameter: Dynamic Modulus*. Publication FHWA-HRT-10-035. Washington, D.C.: Federal Highway Administration.
- LaCroix, A. T., Y. R. Kim, and S. R. Ranjithan. 2008. "Backcalculation of Dynamic Modulus from Resilient Modulus of Asphalt Concrete with an Artificial Neural Network." *Transportation Research Record: Journal of the Transportation Research Board* 2057: 107–113.
- Mahoney, J. 1995. *WSDOT Pavement Guide, Volume 2: Pavement Notes*. Olympia: Washington State Department of Transportation.
- Miller, J. S. and W. Y. Bellinger. 2003. *Distress Identification Manual for the Long-Term Pavement Performance Program*. Revised fourth edition. Publication FHWA-RD-03-031. Washington, D.C.: Federal Highway Administration.
- Nichols Consulting Engineers, Chtd. 1997. *Arizona SPS-9P: Construction Report on Site 040900/04A900*. Federal Highway Administration.
- Perera, R. W. and S. D. Kohn. 2005. *Quantification of Smoothness Index Differences Related to Long-Term Pavement Performance Equipment Type*. Publication FHWA-HRT-05-054. McLean, VA: Federal Highway Administration.
- Puccinelli, J., S. Karamihas, K. Hall, and K. Senn. 2012. *Performance Evaluation of Arizona's LTPP SPS-1 Project: Strategic Study of Flexible Pavement Structural Factors*. FHWA-AZ-12-396. Phoenix: Arizona Department of Transportation.

- Rada, G. R., C. L. Wu, R. K. Bhandari, A. R. Shekharan, G. E. Elkins, and J. S. Miller. 1999. *Study of LTPP Distress Data Variability, Volume I*. Publication FHWA-RD-99-074. Washington, D.C.: Federal Highway Administration.
- Sayers, M. W. 1989. "Two Quarter-Car Models for Defining Road Roughness: IRI and HRI." *Transportation Research Record: Journal of the Transportation Research Board* 1215: 165–172.
- Sayers, M. W. 1990. "Profiles of Roughness." *Transportation Research Record: Journal of the Transportation Research Board* 1260: 106–111.
- Sayers, M. W. and S. M. Karamihas. 1996a. "Estimation of Rideability by Analyzing Longitudinal Road Profile." *Transportation Research Record: Journal of the Transportation Research Board* 1536: 110–116.
- Sayers, M. W. and S. M. Karamihas. 1996b. *Interpretation of Road Roughness Profile Data*. Publication FHWA-RD-96-101 Washington, D.C.: Federal Highway Administration.
- Sebaaly, P. E., Z. Eid, and J. A. Epps. 2001. *Evaluation of Moisture Sensitivity Properties of ADOT Mixtures on US 93*. FHWA-AZ98-402-01. Phoenix: Arizona Department of Transportation.

APPENDIX: ROUGHNESS VALUES

This appendix lists the left International Roughness Index (IRI), right IRI, mean roughness index (MRI), Half-car Roughness Index (HRI), and Ride Number (RN) values for each visit of each section. The roughness values are the average for five repeat runs. The five runs were selected from a group of as many as nine by automated comparison of profiles, as described in the report. Values of standard deviation are also provided for left and right IRI to reveal cases of high variability among the five measurements. However, the screening procedure used to select five repeats usually helped reduce the level of scatter.

The discussion of roughness in the report emphasizes the left and right IRI. Nevertheless, the other indexes do provide useful additional information. MRI is simply the average of the left and right IRI values. HRI is calculated by converting the IRI filter into a half-car model (Sayers 1989) by collapsing the left and right profiles into a single profile in which each point is the average of the corresponding left and right elevations. The IRI filter is then applied to the resulting signal. The HRI is very similar to the IRI except that side-to-side deviations in profile are eliminated. The result is that the HRI value for a pair of profiles will always be lower than the corresponding MRI value. Comparing the HRI and MRI values provides a crude indication of the significance of roll (i.e., side-to-side profile variation) in the overall roughness measurement. When HRI is much lower than MRI, roll is significant. This is common among asphalt pavements (Karamihas et al. 1995). Certain types of pavement distress, such as longitudinal cracking, may also cause significant differences between HRI and MRI.

Figure 24 compares the HRI and MRI for all of the profile measurements that are covered in this appendix (225 pairs of roughness values). The figure shows a best fit line with a zero intercept and a line of equality. The slope of the line is 0.773. This is an unusually large difference between HRI and MRI. Note that a better linear fit was found without forcing a zero intercept. A simple linear fit produced a slope of about 0.711 and an intercept of about 4.6 inches/mi.

RN has shown a closer relationship to road user opinion than the other indexes (Sayers and Karamihas 1996a). As such, it may help distinguish the segments from each other by ride quality. Further, the effect on RN may help quantify the impact of that distress on ride when a particular type of distress dominates the roughness of a section. In particular, a very low RN value coupled with moderate IRI values indicates a high level of short-wavelength roughness and potential sensitivity to narrow dips and measurement errors caused by coarse surface texture.

Table 20 provides the roughness values. The table also lists the date of each measurement and the time in years since the site was opened to traffic. Negative values indicate measurements that were made before rehabilitation.

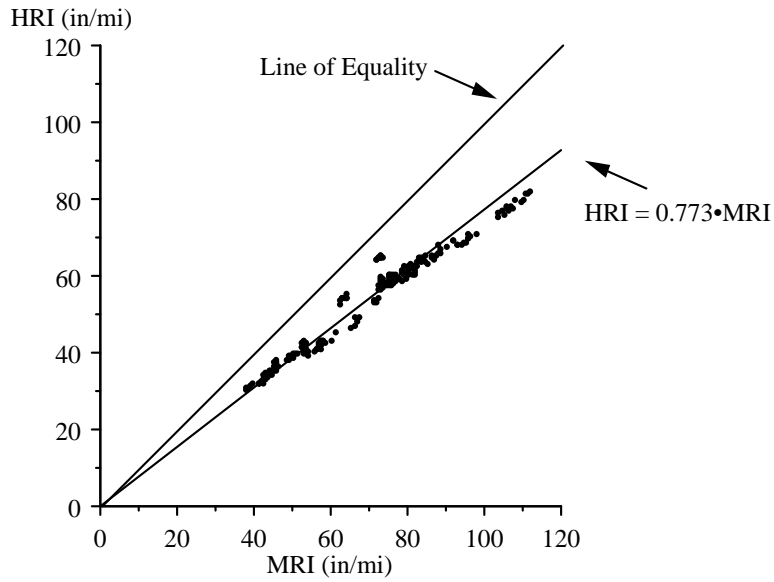


Figure 24. Comparison of HRI to MRI

Table 20. Roughness Values

Section	Date	Years	Left IRI (inches/mi)		Right IRI (inches/mi)		MRI (inch/mi)	HRI (inch/mi)	RN
			Avg.	St. Dev.	Avg.	St. Dev.			
040902	27-Jan-94	0.49	48	1.0	50	0.6	49	39	4.05
	27-Feb-95	1.57	50	0.9	50	0.6	50	40	4.10
	23-Jan-97	3.48	53	0.6	53	0.3	53	41	3.96
	8-Apr-98	4.68	62	2.9	55	1.3	59	43	3.70
	4-Dec-98	5.34	57	0.8	54	1.3	56	41	3.77
	17-Nov-99	6.29	59	0.7	56	0.5	57	43	3.84
	19-Dec-00	7.38	59	0.9	55	0.3	57	43	3.77
	20-Feb-02	8.56	74	0.9	59	1.0	66	48	3.50
	10-Mar-04	10.61	67	0.7	59	1.0	63	54	3.75
27-Mar-06	12.65	66	0.5	60	1.2	63	54	3.75	
040903	23-Jan-97	3.48	87	0.9	58	0.4	73	57	3.85
	8-Apr-98	4.68	96	3.0	63	0.5	79	61	3.48
	4-Dec-98	5.34	91	1.0	61	0.6	76	59	3.58
	17-Nov-99	6.29	84	0.9	64	0.7	74	58	3.65
	19-Dec-00	7.38	82	0.4	64	0.7	73	58	3.61
	20-Feb-02	8.56	82	0.3	69	0.9	75	59	3.42
	9-Mar-04	10.60	83	2.3	73	2.8	78	60	3.13
	27-Mar-06	12.65	85	3.2	77	2.2	81	63	2.95

Table 20. Roughness Values (cont.)

Section	Date	Years	Left IRI (inches/mi)		Right IRI (inches/mi)		MRI (inch/ mi)	HRI (inch/ mi)	RN
			Avg.	St. Dev.	Avg.	St. Dev.			
04A901	27-Feb-95	1.57	35	1.6	42	0.7	38	31	4.27
	23-Jan-97	3.48	37	0.4	46	0.6	41	32	4.23
	8-Apr-98	4.68	37	0.7	49	0.3	43	34	4.10
	4-Dec-98	5.34	37	0.6	48	0.4	43	34	4.16
	17-Nov-99	6.29	40	0.6	47	1.1	44	35	4.17
	19-Dec-00	7.38	38	0.9	48	0.3	43	34	4.24
	20-Feb-02	8.56	43	0.8	48	0.3	45	37	4.16
	10-Mar-04	10.61	43	0.7	48	1.0	45	37	3.98
	27-Mar-06	12.65	53	0.9	53	0.7	53	43	3.80
04A902	27-Jan-94	0.49	73	1.1	73	1.0	73	60	3.70
	27-Feb-95	1.57	74	1.1	77	0.9	76	60	3.75
	23-Jan-97	3.48	76	2.0	82	1.7	79	61	3.65
	8-Apr-98	4.68	81	2.1	89	1.4	85	64	3.39
	4-Dec-98	5.34	72	0.5	88	1.8	80	60	3.57
	17-Nov-99	6.29	75	1.6	90	1.3	83	64	3.52
	19-Dec-00	7.38	75	0.6	92	1.1	84	65	3.51
	20-Feb-02	8.56	79	0.8	96	1.1	87	66	3.45
	10-Mar-04	10.61	75	0.1	69	0.8	72	65	3.76
27-Mar-06	12.65	75	0.9	70	0.4	73	65	3.75	
04A903	23-Jan-97	3.48	71	0.7	72	0.6	71	54	3.73
	8-Apr-98	4.68	78	1.5	85	1.9	82	62	3.38
	4-Dec-98	5.34	82	1.4	98	2.5	90	69	3.34
	17-Nov-99	6.29	90	1.5	98	1.9	94	69	3.36
	19-Dec-00	7.38	92	1.2	99	1.1	96	70	3.31
	20-Feb-02	8.56	101	1.1	111	1.5	106	77	2.99
	9-Mar-04	10.60	98	2.9	111	1.7	105	78	2.90
27-Mar-06	12.65	108	1.1	113	1.3	111	81	2.71	

